



universität
wien

DIPLOMARBEIT

Titel der Diplomarbeit

Generation of Tick-Borne Encephalitis Virus with Mutations in the Fusion Protein E

Verfasserin

Janja Blazevic

angestrebter akademischer Grad

Magistra der Naturwissenschaften (Mag.rer.nat.)

Wien, 2011

Studienkennzahl lt. Studienblatt:

A 490

Studienrichtung lt. Studienblatt:

Diplomstudium Molekulare Biologie

Betreuerin / Betreuer:

Ass.-Prof. Priv.-Doz. Mag. Dr. Karin Stiasny

Dankeschön!

Ein herzliches Dankeschön an Prof. Dr. Franz X. Heinz für die Möglichkeit diese Diplomarbeit am Department für Virologie absolvieren zu können. Dr. Karin Stiasny gilt ein ganz besonderer Dank für die hilfreichen Diskussionen und speziell für die großartige Unterstützung während des Verfassens dieser Arbeit!

Ein weiteres Dankeschön an alle Laborkollegen für die tolle Zusammenarbeit, wobei Dr. Christian Taucher ein besonderer Dank für die tolle Betreuung in der Anfangsphase gilt.

Posebno želim da se zahvalim svojim roditeljima, Ruži i Peji koji su mi omogućili školovanje i koji su imali razumijevanje i strpljenje za mene i moje školovanje.

Hvala najljepše!

Vielen lieben Dank ...

... an meine Schwestern, Bozica, Ilijana und Anna, die mich immer unterstützt haben und ein offenes Ohr für mich hatten!

Danke auch an alle Freunde mit deren Motivation einiges wesentlich leichter fiel!

Table of contents

1	Abstract.....	7
	Zusammenfassung.....	9
2	Introduction	11
2.1	Flaviviridae.....	11
2.2	Epidemiology and disease.....	12
2.3	Molecular biology of flaviviruses	13
2.3.1	Genome structure and translation	13
2.3.2	Flavivirus particles	14
2.3.3	Structural proteins.....	15
2.3.4	Surface structure of flaviviruses.....	18
2.3.5	Subviral particles	18
2.3.6	Flavivirus life cycle.....	19
2.4	Membrane fusion	21
2.4.1	Classification of membrane fusion proteins.....	21
2.4.2	Flavivirus membrane fusion.....	22
3	Objectives	29
3.1	Analysis of the functional relevance of the transmembrane hairpin of flavivirus in membrane fusion	29
3.2	Investigation of key residues of the E protein involved in triggering membrane fusion	30
4	Materials and Methods.....	31
4.1	Materials	31
4.1.1	Cells.....	31
4.1.2	Viruses.....	31
4.1.3	Plasmids	31
4.2	Methods	31
4.2.1	Cloning of transmembrane hairpin mutants.....	31
4.2.2	Cloning of DI/DIII interface mutants.....	32
4.2.3	Agarose gel electrophoresis	33

4.2.4	DNA sequencing.....	33
4.2.5	In vitro RNA transcription.....	33
4.2.6	Transfection of BHK-21 cells by electroporation	34
4.2.7	Infection of BHK-21 cells	34
4.2.8	Viral RNA isolation from supernatant and cDNA synthesis	34
4.2.9	Immunofluorescence staining.....	35
4.2.10	Quantitative TBEV protein E four-layer ELISA	35
4.2.11	Rate zonal gradient centrifugation of viral particles.....	35
4.2.12	RNA quantification by real-time PCR analysis.....	36
4.2.13	Focus formation assay.....	36
5	Results.....	37
5.1	Analysis of the functional relevance of the transmembrane hairpin of flavivirus in membrane fusion	37
5.1.1	Generation of full-length cDNA clones.....	37
5.1.2	Characterization of mutant viruses	39
5.2	Investigation of key residues of the E protein involved in triggering membrane fusion	46
5.2.1	Generation of full-length cDNA clones.....	46
5.2.2	Characterization of mutant viruses	49
6	Discussion.....	55
6.1	Analysis of the functional relevance of the transmembrane hairpin of flavivirus in membrane fusion	55
6.2	Investigation of key residues of the E protein involved in triggering membrane fusion	56
7	References.....	58
	Appendix	62
	Curriculum Vitae.....	71

1 Abstract

Membrane fusion is a crucial step during the cell entry of enveloped viruses and is driven by specific membrane-anchored viral surface proteins (fusion proteins). According to their molecular architecture these proteins have been assigned to three different structural classes (class I, II, and III). They all drive fusion by conformational changes that are triggered by interactions with the host cell (such as receptor binding or exposure to acidic pH) and presumably involve protein-protein interactions at the fusion site.

Flaviviruses are small enveloped viruses and comprise several human pathogens like yellow fever virus, dengue virus, Japanese encephalitis virus (JEV), West Nile virus, and tick-borne encephalitis virus (TBEV). These viruses enter the host cells by receptor mediated endocytosis followed by fusion in the endosome mediated by the envelope protein E, a class II viral fusion protein. The acidic pH in the endosome triggers the conformational reorganization from metastable pre-fusion E homodimers into post-fusion trimers. The crystal structures of truncated E proteins, lacking the so-called 'stem'-region and the membrane anchor, are known in their pre- and post-fusion conformations. The E protein is the only known viral fusion protein with a double membrane anchor, consisting of two antiparallel transmembrane helices (TM1 and TM2), required for intracellular sorting and processing of the viral polyprotein. Using recombinant subviral particles (RSPs) of TBEV with truncated and chimeric forms of protein E (containing heterologous JEV TM segments) it was shown that both TM helices are essential for efficient fusion. Functional analyses demonstrated that TM interactions apparently contribute to the stability of the post-fusion trimer and the completion of the merger of the membranes.

In this diploma thesis we were interested to assess the significance of the observations made with RSP TM mutations in the context of infectious virions, heterologous and chimeric membrane anchors were introduced into an infectious cDNA clone of TBEV. The studies revealed that recombinant TBE viruses with a completely heterologous TM anchor or chimeric TM anchors had dramatically reduced specific infectivities. They were also severely impaired in their virus growth properties thus prohibiting the production of sufficient amounts of mutant viruses for in vitro fusion experiments. The data obtained in this work suggest that modifications of the TM helices in the virus not only affected fusion, but also additional steps of the virus life cycle such as particle assembly.

In the second part of this diploma thesis, the role of conserved histidines in the E protein as pH sensors for triggering flavivirus membrane fusion were analysed in the context of infectious TBEV. A previous study using TBEV RSPs revealed that one histidine at an interface between two domains was important for the acidic-pH-induced initiation of fusion and a second histidine at this interface (which could not be investigated with RSPs) was

speculated to be also involved in this process. Replacement of these histidines in infectious TBE virions led to a 10-fold reduced infectivity of the mutants compared to wild type and the combination of both mutants yielded even a 100-fold reduced infectivity. The generation of these mutants now provides the basis for further experiments to analyze the pH sensor in an infectious system, including the determination of specific infectivities and fusion activities of the histidine mutants after up-scaling of virus productions.

Zusammenfassung

Die Membranfusion ist ein essentieller Schritt im Infektionsprozess umhüllter Viren und wird durch spezifische membranverankerte virale Oberflächenproteine (Fusionsproteine) vermittelt. Auf Grund ihres molekularen Aufbaus werden diese Proteine in drei unterschiedliche strukturelle Klassen eingeteilt (Klasse I, II und III). Sie alle bewirken Fusion durch Konformationsänderungen, die durch Interaktionen mit der Wirtszelle (wie z.B. Rezeptorbindung oder sauren pH) ausgelöst werden, wobei vermutlich Protein-Protein Wechselwirkungen am Fusionsort beteiligt sind.

Flaviviren sind umhüllte Viren, die eine Reihe von humanen Pathogenen umfassen wie Gelbfieber Virus, Dengue Virus, Japanische Enzephalitis Virus (JEV), West Nil Virus und Frühsommer-Meningoenzephalitis Virus (FSMEV). Diese Viren dringen durch rezeptorvermittelte Endozytose und anschließende Fusion ihrer Membran und der endosomalen Membran in Wirtszellen ein. Das Hüllprotein E („envelope“), ein virales Klasse II Fusionsprotein, ist für den Fusionsprozess verantwortlich. Der saure pH Wert der Endosomen löst die konformationelle Reorganisation vom metastabilen E Homodimeren in post-Fusions-Trimere aus. Die Kristallstrukturen von löslichen verkürzten E Proteinen verschiedener Flaviviren, denen die sogenannte „Stamm“-Region und der doppelte Membrananker fehlen, wurden vor und nach der säure-induzierten Umlagerung geklärt. Bemerkenswert ist, dass das E Protein als einziges bekanntes virales Fusionsprotein einen doppelten Transmembrananker besitzt, der aus zwei antiparallel angeordneten Transmembranhelices (TM1 und TM2) besteht. Diese sind für das intrazelluläre Sortieren und Prozessieren des viralen Polyproteins erforderlich.

Unter Verwendung von rekombinanten subviralen Partikeln (RSP) des FSME Virus, die verkürzte und chimäre (mit heterologen JEV TM Segmenten) Formen des E Proteins enthalten, konnte gezeigt werden, dass beide TM Helices für eine effiziente Fusion notwendig sind. Funktionelle Analysen wiesen darauf hin, dass TM Interaktionen offenbar zur Stabilität des post-Fusions-Trimer und zur Vervollständigung des Fusionsprozesses der beiden Membranen beitragen.

Ziel dieser Diplomarbeit war es, die Bedeutung der Beobachtungen mit RSP TM Mutationen im infektiösen FSMEV System zu verifizieren. Hierfür wurden heterologe und chimäre Membrananker in infektiöse FSMEV cDNA Klone eingebracht. Rekombinante FSME Viren mit einem gänzlich heterologen TM Anker oder chimären TM Ankern zeigten eine dramatische Reduktion der spezifischen Infektiösität und eine starke Beeinträchtigung der Virusvermehrung. Dadurch war es nicht möglich, mutierte Viren in ausreichender Menge für in vitro Fusionsexperimente herzustellen. Die in dieser Diplomarbeit gewonnene Daten deuten darauf hin, dass Modifikationen der TM Helices im Virus nicht nur die Fusion

beeinflussen, sondern auch zusätzliche Schritte des viralen Lebenszyklus wie Partikel Aufbau („Assembly“) betreffen.

Im zweiten Teil dieser Diplomarbeit sollte die Funktion von konservierten Histidinen im E Protein als pH Sensoren für die Flavivirus Membranfusion in infektiösen FSME Viren analysiert werden. Eine vorangegangene Studie unter Verwendung von FSMEV RSPs hatte gezeigt, dass ein Histidin an der Schnittstelle zwischen zwei Domänen für die saure pH-induzierte Einleitung der Fusion wichtig ist. Es wurde spekuliert, dass ein zweites Histidin in dieser Region (welches jedoch im RSP System nicht untersucht werden konnte) ebenfalls an diesem Prozess beteiligt sein könnte. Der Austausch eines dieser Histidine führte in FSME Viren zu einer 10-fachen Reduktion der Infektiosität der Mutanten im Vergleich zum Wildtyp und die Kombination der beiden Mutanten ergab sogar eine 100-fache Reduktion der Infektiosität. Die Produktion dieser Mutanten liefert nun die Grundlage für weitere Studien einschließlich der Analyse der spezifischen Infektiosität und Fusionsaktivität nach Virusproduktion im Großmaßstab, um die Funktion von Histidine als pH Sensoren im infektiösen System untersuchen zu können.

2 Introduction

2.1 Flaviviridae

Flaviviridae represent a large family of small, enveloped RNA viruses that are classified into three genera: the genus *Flavivirus*, the genus *Hepacivirus*, and the genus *Pestivirus*. Members of this family share similarities in virion morphology, genome organization, and replication strategy (Lindenbach 2007).

Flavivirus is the largest genus of this family and comprises more than 70 virus species (Fauquet 2005; Mukhopadhyay, Kuhn et al. 2005). Most of them are arthropod-borne viruses and are transmitted by mosquitoes or ticks. For some flaviviruses the transmission is not known and most probably does not involve an arthropod vector (Fauquet 2005).

This genus can be subdivided into serological (corresponding to serocomplexes) and phylogenetical (based on clades and clusters) groups, as shown in Figure 1 (Kuno, Chang et al. 1998).

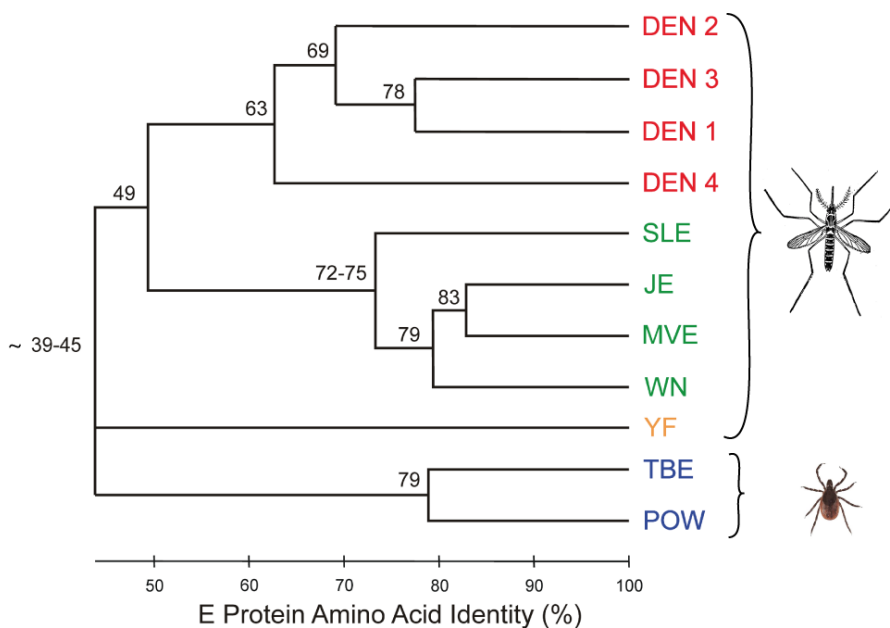


Figure 1: Flavivirus classification

The dendrogram represents the relationship between the flaviviruses based on amino acid identity in the E protein. The classification of flaviviruses into serocomplexes is indicated by different colors: dengue virus serocomplex is represented in red, Japanese encephalitis virus serocomplex in green, yellow fever virus serocomplex in orange, and tick-borne encephalitis virus serocomplex in blue. The brackets on the right show the mosquito-borne and tick-borne virus clusters. Dengue virus (DEN), St. Louis encephalitis (SLE) virus, Japanese encephalitis (JE) virus, Murray Valley encephalitis (MVE) virus; West Nile (WN) virus, yellow fever (YF) virus, tick-borne encephalitis (TBE) virus, Powassan (POW) virus. Figure modified from (Stiasny, Kiermayr et al. 2006).

Important human flavivirus pathogens are dengue virus (DENV), Japanese encephalitis virus (JEV), tick-borne encephalitis virus (TBEV), West Nile virus (WNV), and yellow fever virus (YFV) (Gubler 2007).

Tick-borne encephalitis viruses can be classified as one species with three subtypes: Far Eastern, Siberian and European subtype (Ecker, Allison et al. 1999; Fauquet 2005).

2.2 Epidemiology and disease

Tick-borne encephalitis virus

Tick-borne encephalitis virus is endemic in regions of Europe and Asia and its main transmission vectors are ticks. The European TBEV subtype is mainly transmitted by *Ixodes ricinus*, the other two subtypes by *Ixodes persulcatus* (Gubler 2007; Lindquist and Vapalahti 2008). The natural hosts of TBEV are ticks and small vertebrates, mainly rodents, although larger animals like deer can get infected as well. Approximately 3,000 hospitalized human cases are reported annually in Europe and up to 10,000 in Russia (Donoso Mantke, Schadler et al. 2008). Typically, the disease takes a biphasic course. After an asymptomatic period of several days, the second phase with central nervous system symptoms, such as meningitis, meningoencephalitis, meningoencephalomyelitis, or meningoencephaloradiculitis, occurs in 20-30% of infected humans (Haglund and Gunther 2003; Holzmann 2003; Lindquist and Vapalahti 2008). The available vaccines licensed for use in Europe contain highly purified formalin-inactivated European TBEV strains adsorbed to aluminium hydroxide (Barrett 2008). The field effectiveness of TBEV vaccines is > 95% (Heinz, Holzmann et al. 2007).

Japanese encephalitis virus

Japanese encephalitis virus is the leading recognized cause of viral encephalitis in eastern, southern and southeastern Asia and Papua New Guinea. 30,000-50,000 clinical cases per year are recorded and of these about 25-30% are fatal and about 50% result in neurological sequelae (Mackenzie, Gubler et al. 2004). Clinical disease varies from a nonspecific febrile illness to meningoencephalitis, aseptic meningitis or a polio-like acute flaccid paralysis (Solomon and Vaughn 2002). JE virus exists in a zoonotic transmission cycle between mosquitoes and pigs and/or water birds. The transmission to humans occurs only incidentally by the bite of an infected mosquito and humans are dead-end hosts (Mackenzie, Gubler et al. 2004). Available vaccines for immunization against JEV are either killed vaccines containing formalin-inactivated JEV or a live-attenuated vaccine (JE SA 14-14-2) in China (Fischer, Casey et al. 2007).

2.3 Molecular biology of flaviviruses

2.3.1 Genome structure and translation

The flavivirus genome is a linear, single-stranded, positive-sense RNA of about 11 kb. The genome contains a single open reading frame (ORF) that is flanked by 5' and 3' noncoding regions (NCRs) (Figure 2A). The NCRs form specific secondary structures that play an important role in genome replication and translation (Lindenbach 2007).

The genomic RNA is translated into an about 3400 amino acid long polyprotein which is co- and post-translationally processed by a combination of viral and host proteases. It gives rise to ten viral proteins. The N-terminal part contains the structural proteins followed by seven non-structural proteins. The capsid (C), the precursor of membrane glycoprotein (prM) and the envelope (E), form the virus particle. The non-structural proteins, NS1, NS2A, NS2B, NS3, NS4A, NS4B, and NS5, are essential for replication of the viral genome (Lindenbach 2007).

During translation of the polyprotein, the viral proteins are translocated and anchored in the endoplasmic reticulum (ER). The topology of viral surface proteins – with respect to the endoplasmic reticulum – is defined by stop-transfer and signal sequences.

The capsid protein has a signal sequence at the carboxy-terminus, which is responsible for recruiting prM into the ER lumen. The prM protein is anchored in the ER membrane by two transmembrane helices, whereof the second serves as a signal sequence for the E protein and an ER-retention signal (Mukhopadhyay, Kuhn et al. 2005). The E Protein is anchored as well in the ER membrane by two transmembrane helices, whereof the second segment is an internal signal sequence for NS1. The E/NS1 junction is cleaved by a host signal peptidase resulting in the release of NS1 into the lumen of the ER (Lindenbach 2007). The topology of the viral structural proteins and the cleavage sites for the proteases are shown in Figure 2B.

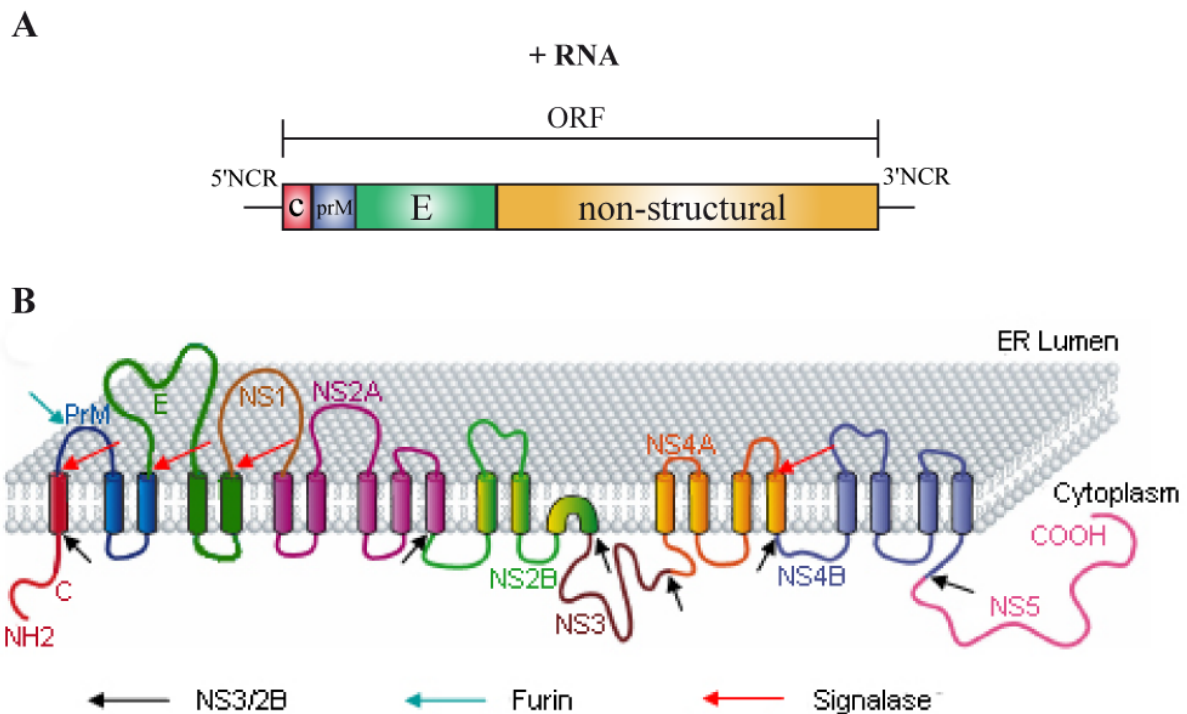


Figure 2: Flavivirus genome structure and membrane topology of the viral proteins

(A) Schematic of the TBEV genome: The TBEV genome consists of a linear, positive-sense RNA with a single open reading frame (ORF). The genome encodes 10 proteins: The structural proteins in the order C, prM/M and E, followed by seven non-structural proteins in the order NS1, NS2A, NS2B, NS3, NS4A, NS4B, and NS5. Figure adapted from (Stiasny and Heinz 2006).

(B) Membrane topology of the viral proteins with respect to the endoplasmatic reticulum membrane (grey). The cleavage sites of viral and host derived proteases are indicated by arrows. The viral proteins are shown in different colors. The transmembrane domains of the viral proteins are displayed as cylinders. Figure adapted from (Umareddy, Pluquet et al. 2007).

2.3.2 Flavivirus particles

Flaviviruses are small lipid-enveloped viruses. The nucleocapsid consists of the genomic RNA surrounded by multiple copies of the capsid protein (C). It is surrounded by a lipid bilayer derived from the endoplasmic reticulum of the host cell. Two membrane-anchored proteins, envelope (E) and membrane (M), cover the virion surface (Lindenbach 2007).

Virions are assembled as immature particles, displaying heterodimers of the precursor form of M (prM) and E on their surface (Figure 3). During maturation, the pr peptide of the prM protein is proteolytically cleaved, which leads to structural rearrangements on the viral surface. In mature viral particles, the surface is smooth and completely covered by tightly interacting E homodimers that are oriented parallel to the virus surface (Figure 3).

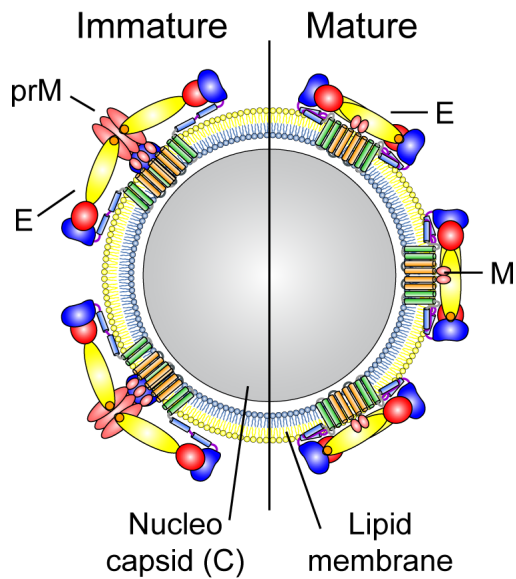


Figure 3: Schematic illustration of immature and mature flavivirus particles

Immature virion with prM and E heterodimers (left); mature form after proteolytic cleavage of prM during maturation with M proteins and E homodimers (right). Figure adapted from (Stiasny and Heinz 2006).

2.3.3 Structural proteins

2.3.3.1 Capsid protein

The capsid protein (C) is the smallest flavivirus structural protein with a size of 12-14 kDa, playing an essential role in virus assembly and encapsidation of the viral genome (Mukhopadhyay, Kuhn et al. 2005). It contains a number of basic residues, accumulated at the C- and N-termini, and an internal hydrophobic region.

The C protein monomer contains four alpha helices that are linked by short loops. Two capsid protein monomers build a compact dimer. For the assembly of the nucleocapsid, positively charged residues of the C protein bind to the negatively charged RNA and the hydrophobic residues interact with the viral membrane (Lindenbach 2007).

2.3.3.2 Membrane Glycoprotein

The membrane precursor of M (prM) is about 26 kDa and contains up to three N-linked glycosylation sites and six conserved cysteins, which form disulfide bridges (Nowak, Farber et al. 1989; Chambers, Hahn et al. 1990). The two transmembrane domains consist of two antiparallel coiled coils, which anchor the prM protein in the host-derived membrane (Zhang, Chipman et al. 2003).

PrM acts as a chaperone for the E protein folding and is involved in the formation of prM-E heterodimers in immature particles (Allison, Stadler et al. 1995; Lorenz, Allison et al. 2002). The main function of prM is the prevention of low-pH-induced rearrangements of the fusion protein E, that would lead to premature fusion during exocytosis (see 2.2.6) (Stadler, Allison et al. 1997; Lindenbach 2007).

Particle maturation occurs in the trans-Golgi-network (TGN) where the low pH induces conformational changes in the prM/E glycoproteins complexes leading to the exposure of the furin cleavage site (Stadler, Allison et al. 1997). After secretion of the virus into the extracellular space, the neutral pH triggers the release of the pr part resulting in mature particles (Yu, Zhang et al. 2008).

The mature M protein is the smaller part of the prM original protein and consists of only 75 amino acids. Whether it has a specific function still remains elusive (Mukhopadhyay, Kuhn et al. 2005).

2.3.3.3 Envelope Glycoprotein

The flavivirus envelope protein E, a class II viral fusion protein (53 kDa), mediates receptor binding and membrane fusion (Kielian 2006; Stiasny and Heinz 2006). It contains 12 conserved cysteins that form six disulfide bonds (Nowak 1987). On mature virions the E protein is arranged in head-to-tail homodimers that are oriented parallel to the viral membrane.

Each E monomer is composed of the E protein ectodomain, the stem region, and the membrane anchor (Zhang, Chipman et al. 2003) (Figure 4B).

The atomic structures of the ectodomains (soluble E, sE) of several flaviviruses have been determined (Rey, Heinz et al. 1995; Modis, Ogata et al. 2003; Zhang, Zhang et al. 2004; Modis, Ogata et al. 2005; Kanai, Kar et al. 2006; Nybakken, Nelson et al. 2006).

The E ectodomain is organized in three domains (DI, DII, and DIII) and is shown in Figure 4A: the central domain I forms a β -barrel, the elongated domain II is responsible for dimerisation, and domain III, which maintains an immunoglobulin-like fold, is involved in receptor binding (Lindenbach 2007). The three domains are connected with flexible junctions (Modis, Ogata et al. 2003; Zhang, Zhang et al. 2004) that enable the E protein to undergo structural rearrangements.

Domain II of the E protein contains a hydrophobic highly conserved sequence element at its tip, the fusion peptide (FP). The FP is of central importance for interactions with the host cell membranes during viral membrane fusion (Allison, Schalich et al. 2001).

The stem region contains two amphipathic α -helices (H1 and H2), which are arranged parallel to the outer leaflet and half-buried in the viral membrane (Zhang, Chipman et al. 2003).

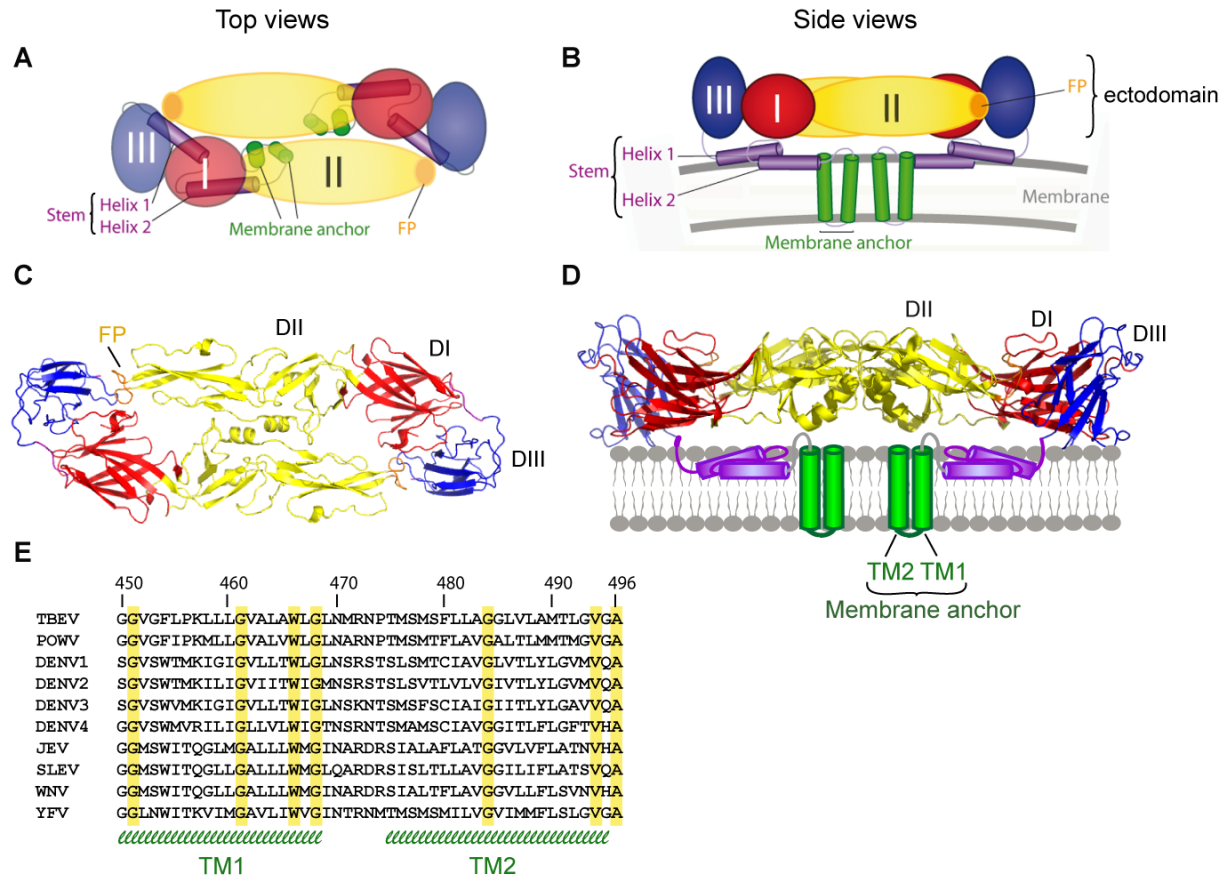


Figure 4: Representations of flavivirus protein E in its pre-fusion conformation and conserved residues in the membrane anchor of E

(A,B) Schematics of the full-length E dimer. Figure modified from (Kiermayr, Stiasny et al. 2009). (C,D) Ribbon diagrams of the TBEV protein E ectodomain. The stem and anchor regions are shown schematically as cylinders. Color codes: DI, red; DII, yellow; DIII, blue; FP, orange; helices of the stem, purple; C-terminal transmembrane helices, green; lipid membrane, grey. Figure modified from (Stiasny and Heinz 2006). (E) Alignment of the amino acid sequences of the transmembrane regions of several flaviviruses (TBEV numbering): TBEV (Gene bank accession number U27495), Powassan virus (POWV) (Gene bank accession number FJ687432), DENV type 2 (Gene bank accession number NC_001474), DENV type 3 (Gene bank accession number FJ850055), DENV type 4 (Gene bank accession number AY618990), JEV (EF571853), St. Louis encephalitis virus (SLV) (Gene bank accession number M16614), West Nile virus (WNV) (Gene bank accession number DQ211652), Yellow fever virus (YFV) (Gene bank accession number AY640589). The predicted TM1 and TM2 helices are indicated at the bottom. Figure modified from (Fritz, Blazevic et al. 2011)

The E protein is anchored in the viral membrane by two transmembrane helices (TM1 and TM2) (Figure 4B). These transmembrane domains (TMDs) result from the polyprotein processing (Figure 2B) and form an antiparallel hairpin structure (Zhang, Chipman et al. 2003). The two TMs are separated by a linker of four to six amino acids (mostly polar) that are located at the cytoplasmic side of the membrane. The TMDs among flaviviruses show low sequence conservation (Figure 4E). The structure of the double membrane anchor is unique for the flavivirus fusion protein and not found in other viral fusion proteins. Its specific functional role was recently investigated in a study by Fritz et al. which showed that TM interactions contribute to the stability of the E protein post-fusion conformation and to the completion of the fusion process (Fritz, Blazevic et al. 2011).

2.3.4 Surface structure of flaviviruses

Mature virions are 50 nm in diameter and have a spikeless and smooth surface. Cryo-electronmicroscopy of mature flavivirus particles revealed an icosahedral particle organization (Mukhopadhyay, Kuhn et al. 2005). At the viral surface 180 E monomers are arranged in a herringbone-like pattern consisting of 30 rafts of three parallel E dimers (Kuhn, Zhang et al. 2002; Mukhopadhyay, Kim et al. 2003) (Figure 5B).

Immature virions have a diameter of about 60 nm (Lindenbach 2007). Newly synthesized virus particles contain 60 trimeric spikes on their virus surface. Each spike consists of 3 E monomers surrounding a prM trimer (Zhang, Zhang et al. 2004; Mukhopadhyay, Kuhn et al. 2005) (Figure 5A).

Recent studies report that not only completely mature and completely immature but also partially mature/immature particles can be secreted from flavivirus infected cells (Cherrier, Kaufmann et al. 2009; Junjhon, Edwards et al. 2010).

2.3.5 Subviral particles

In addition to the secretion of whole virus particles, smaller, non-infectious subviral particles with a diameter of 30 nm can be released from flavivirus infected cells (Stollar 1969; Smith, Brandt et al. 1970) (Figure 5C). These subviral particles are called slowly sedimenting hemagglutinin (SHA). SHA particles contain only the E and prM/M proteins anchored in a lipid membrane, but lack the nucleocapsid (Lindenbach 2007). Such particles can be produced in recombinant form by the coexpression of the viral surface proteins prM and E in mammalian cells (Allison, Stadler et al. 1995; Schalich, Allison et al. 1996). Cryo-electronmicroscopy studies using recombinant subviral particles (RSPs) of TBEV revealed a

T=1 icosahedral symmetry of 30 E dimers at their surface (Ferlenghi, Clarke et al. 2001). Although the particles differ in their architecture compared to the mature virus, RSPs share similar properties with respect to fusion activity (Schalich, Allison et al. 1996; Corver, Ortiz et al. 2000; Mukhopadhyay, Kuhn et al. 2005). These particles have been established as a model system to study fusion of flaviviruses (Allison, Schalich et al. 2001; Fritz, Stiasny et al. 2008).

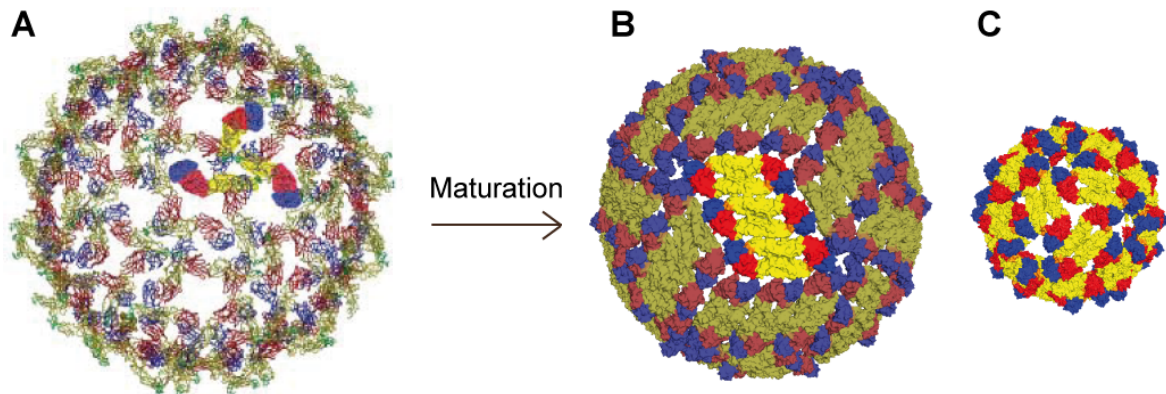


Figure 5: Flavivirus particles and recombinant subviral particle

Structures of (A) immature, (B) mature viral particles and (C) mature RSP based on cryo-electron microscopy reconstructions. (A) One trimeric E protein spike of an immature particle is highlighted. (B) One raft, containing 3 parallel E dimers, is highlighted. Figure (A) and (B) adapted from (Zhang, Zhang et al. 2004; Mukhopadhyay, Kuhn et al. 2005). Figure (C) adapted from (Ferlenghi, Clarke et al. 2001; Kiermayr, Stiasny et al. 2009). Color codes: DI, red; DII, yellow; DIII, blue; for figure A: FP, green; for figure B and C: FP, orange.

2.3.6 Flavivirus life cycle

Flaviviruses attach and bind to poorly characterized receptor molecules on the cell surface. For the initial attachment of several flavivirus to host cells highly sulfated glycosaminoglycans (e.g. heparin sulfate) have been discussed to play an important role (Kroschewski, Allison et al. 2003). The virus is internalized into the target cell by receptor-mediated, clathrin-dependent endocytosis and ends up in the endosome (Kaufmann and Rossmann 2010). The acidic pH of the endosome induces conformational changes in the E protein that mediate fusion of the viral and endosomal membrane. This finally leads to the release of the viral RNA genome into the cytoplasm (Stiasny and Heinz 2006). The viral plus-stranded RNA is directly translated into a single viral polyprotein which is co- and post-translationally cleaved to give rise to the viral proteins (Lindenbach 2007). NS3 and NS5 form the replication complex, together with other viral and host proteins. The replication complex synthesizes a negative-sense RNA that acts as a template for the synthesis of genomic plus-stranded RNA (Lindenbach 2007).

The newly synthesized C protein, located at the cytoplasmic side of the ER, recruits viral genomic progeny RNA. The assembly of viral particles occurs at the ER membrane. The budding into the ER leads to a host-derived lipid envelope of the virus and the formation of immature viral particles (Lindenbach 2007). Protease- and pH-dependent maturation of the viral particle takes place during the transit from the ER through the trans-Golgi-network to the cell surface (Stadler, Allison et al. 1997; Elshuber, Allison et al. 2003; Yu, Zhang et al. 2008). Maturation is responsible for significant E protein reorganization and furin cleavage of prM (Stadler, Allison et al. 1997). After the furin cleavage of prM, the pr fragment stays associated with E (Yu, Zhang et al. 2008) and prevents premature fusion in the acidic trans-Golgi-network during exocytosis (Stadler, Allison et al. 1997). Upon secretion into the extracellular space, the removal of pr is triggered by neutral pH (Yu, Zhang et al. 2008) leading to mature virus particles ready for a new infection (Mukhopadhyay, Kuhn et al. 2005).

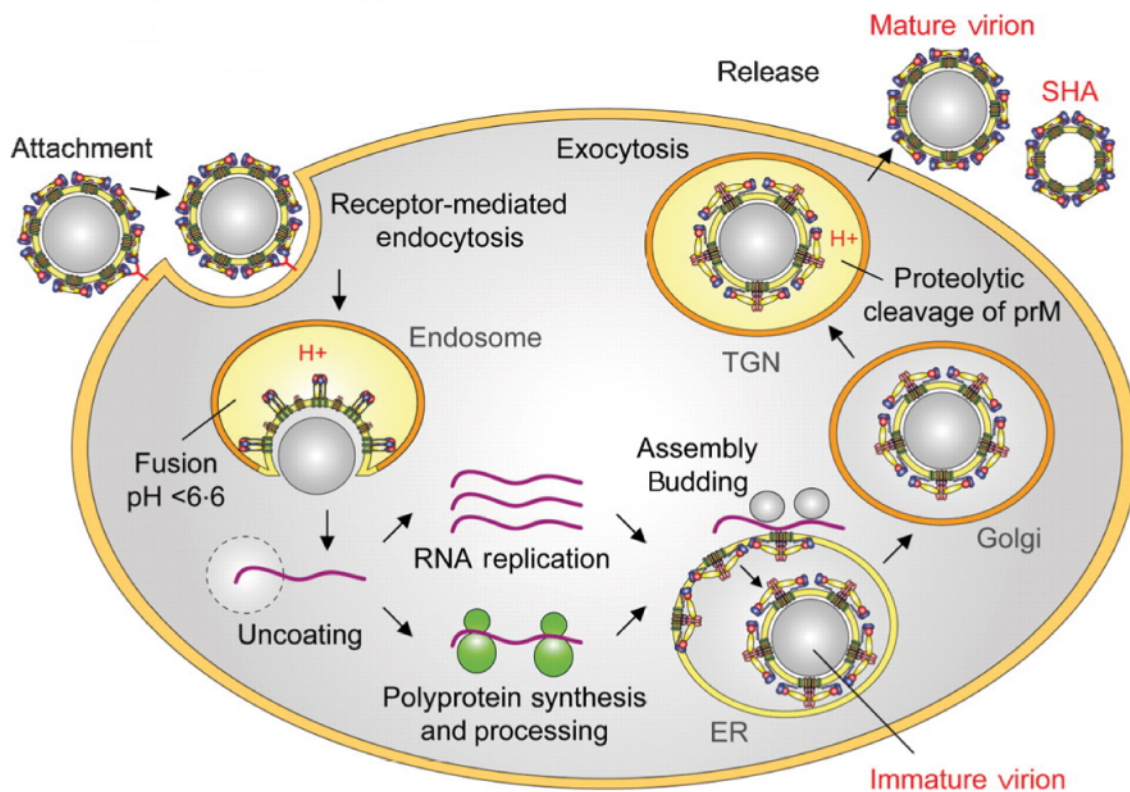


Figure 6: Flavivirus life cycle

Flavivirus entry occurs by receptor mediated endocytosis. The low pH of the endosomes induces structural changes in the E protein leading to fusion and the release of the nucleocapsid into the cytoplasm. Translation and replication of the viral genome occur in the cytoplasm. Viral assembly takes place in the ER. Newly assembled immature virions are transported through the exocytic pathway where maturation cleavage occurs. Mature viral and slowly sedimenting hemagglutinin (SHA) particles are released from infected cells. ER, endoplasmatic reticulum; TGN, trans-Golgi-network. Figure adapted from (Stiasny and Heinz 2006).

2.4 Membrane fusion

Membrane fusion is a fundamental biological process leading to the merger of two separate lipid membranes into a single bilayer (Martens and McMahon 2008). The entry of enveloped viruses into host cells involves membrane fusion and is mediated by viral fusion proteins (Harrison 2008; White, Delos et al. 2008).

Fusion takes place either directly at the plasmamembrane or at the membrane of an intracellular compartment, e.g. endosomes, after endocytotic uptake (Harrison 2008). Fusion proteins are anchored in the viral membrane and primed to undergo structural changes that drive fusion and provide the energy for the fusion process (Stiasny and Heinz 2006; Harrison 2008). These rearrangements are activated by specific triggers and ensure that the fusion process occurs at the right time and the right place of the viral life cycle. Different trigger mechanisms have been described: 1. interactions with receptors (e.g. human immunodeficiency virus, HIV), 2. low pH in the endosomes leading to protonation of fusion relevant residues (e.g. influenza viruses, flaviviruses), and 3. a combination of receptor interaction and low pH (some retroviruses) (White, Delos et al. 2008).

2.4.1 Classification of membrane fusion proteins

Viral surface fusion proteins can be divided into 3 structural classes (Weissenhorn, Hinz et al. 2007; White, Delos et al. 2008).

- Class I fusion proteins are mainly composed of α -helical coiled coil structures and carry N-terminal or N-proximal located FPs. Orthomyxo-, paramyxo-, retro-, filo-, and coronaviruses are representatives for class I fusion proteins (Schibli and Weissenhorn 2004). These proteins share analogies to SNARE proteins involved in cellular fusion processes (Sapir, Avinoam et al. 2008).
- Class II fusion proteins are largely composed of β -sheets and possess internal FPs. They are found in alpha- und flaviviruses (Kielian 2006; Stiasny and Heinz 2006).
- Class III fusion proteins contain mixed secondary structures and share features with class I and II fusion proteins. Fusion proteins of rhabdo-, herpes-, and baculoviruses belong to this class (Backovic and Jardetzky 2009).

2.4.2 Flavivirus membrane fusion

2.4.2.1 Pre- and post-fusion structure of the E protein

In the pre-fusion conformation (described in section 2.3.3.3), two protein E monomers form head-to-tail metastable homodimers which are orientated parallel to the viral membrane and slightly curved (Figure 7A). Within the pre-fusion dimer, the fusion loop is buried in a hydrophobic pocket formed by DI and DIII of the second subunit (Figure 7B) (Rey, Heinz et al. 1995; Modis, Ogata et al. 2003).

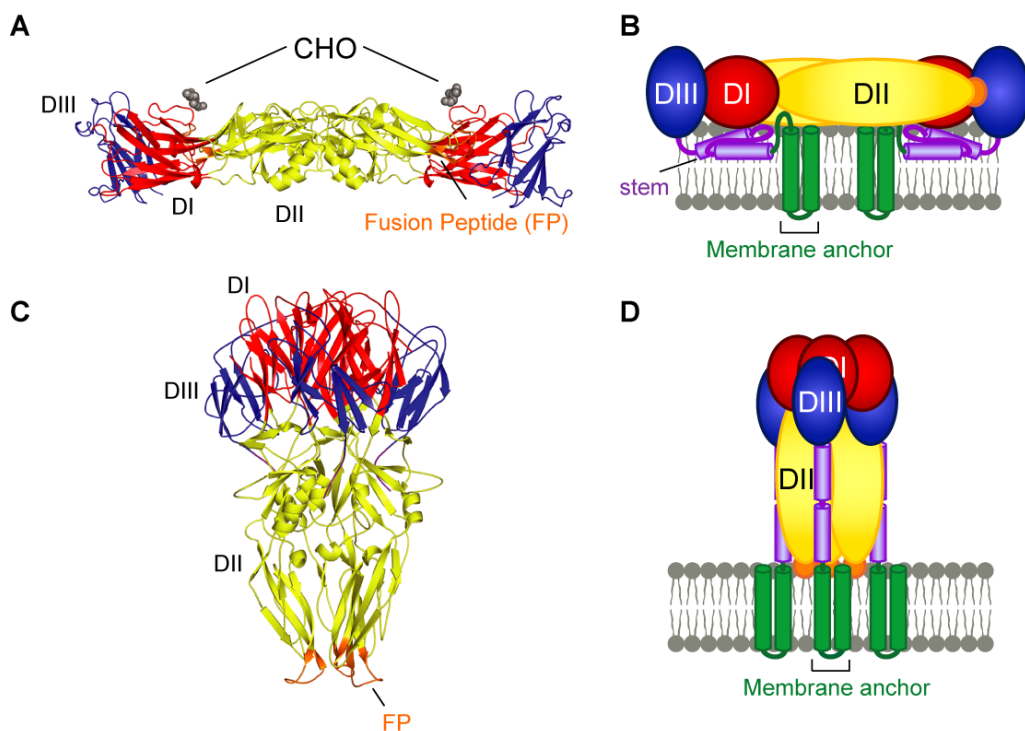


Figure 7: Ribbon diagrams and schematics of TBEV proteins E in their pre- and post-fusion conformations.

Side views of the sE (A) and full-length E (B) dimer in their pre-fusion conformation. Side view of the sE (C) and full-length (D) E post-fusion trimer. The position of the transmembrane domains of the membrane anchor and the helices of the stem are based on the study of (Bressanelli, Stiasny et al. 2004). Color code corresponds to Figure 3. Figure adapted from (Stiasny and Heinz 2006)

During the low-pH-induced fusion process the E protein undergoes a transition from the pre- (Figure 7A, B) to the post-fusion structure (Figure 7C, D). This transition causes an irreversible reorganization of the molecule from a horizontal dimer into a vertically oriented trimer (Bressanelli, Stiasny et al. 2004; Modis, Ogata et al. 2004; Nayak, Dessau et al. 2009). In the post-fusion conformation, the monomeric subunits are oriented parallel to each other. DII is slightly reoriented due to a 20° rotation at the DI-II junction. DIII of E relocates to the

side of DI and points towards DII (Figure 8). This arrangement causes a juxtaposition of the fusion loops and the TMDs on the same side of the molecule (Figure 7D). It is predicted that two neighboring DIIs of the E trimer generates a hydrophobic groove along their interface. The stem regions are supposed to bind this hydrophobic area (Bressanelli, Stiasny et al. 2004) (Figure 7D).

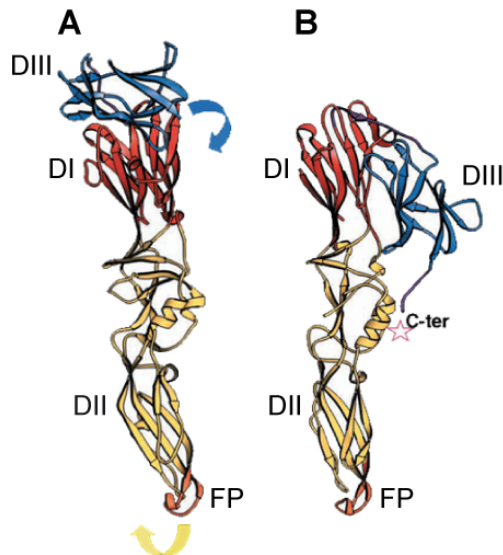


Figure 8: Relocation of DIII of TBEV protein E

Ribbon diagram of the sE protein (A) in their pre-fusion conformation and (B) in their post-fusion conformation. The low-pH-induced movements of DII (yellow arrow) and DIII (blue arrow) are indicated by curved arrows. (B) The position of the C-terminal residue of the crystallized sE fragment is indicated by an open star. Figure adapted from (Bressanelli, Stiasny et al. 2004).

2.4.2.2 Fusion mechanism

Based on the crystal structure of flaviviral sE proteins in their pre- and post-fusion conformation (Rey, Heinz et al. 1995; Modis, Ogata et al. 2003; Bressanelli, Stiasny et al. 2004; Modis, Ogata et al. 2004; Zhang, Zhang et al. 2004; Modis, Ogata et al. 2005; Kanai, Kar et al. 2006; Nybakken, Nelson et al. 2006; Nayak, Dessau et al. 2009) and biochemical studies, a model for flavivirus membrane fusion has been established (Figure 9). The intermediate stages are hypothetical only and need further investigations.

Flaviviruses are taken up by receptor-mediated endocytosis. The internalized virus ends up in endosomes where the acidic pH-dependent membrane fusion occurs.

Acidic-pH-induces first a dissociation of the metastable pre-fusion E homodimers into monomers (Stiasny, Kossel et al. 2007) (Figure 9A), thereby leading to the exposure of the FP loops at the tip of DII (Stiasny, Allison et al. 2002). The fusion peptides insert into the target

membrane (Figure 9B) followed by the trimerization of E and relocation of DIII to the side of the molecule (Stiasny and Heinz 2006) (Figure 9C). This rearrangement is possible by flexible junctions between the domains (Stiasny and Heinz 2006).

Fusion proceeds by the zippering of the stem along the body of the trimer (Figure 9D). The formation of the hairpin-like post-fusion trimer with the fusion peptides and the membrane anchor at the same side of the molecule finally leads to the opening of the fusion pore (Figure 9E).

The transition from the metastable E homodimers into more stable E homotrimers provides the energy to overcome the kinetic barrier for merging the two membranes (Stiasny and Heinz 2006; Harrison 2008).

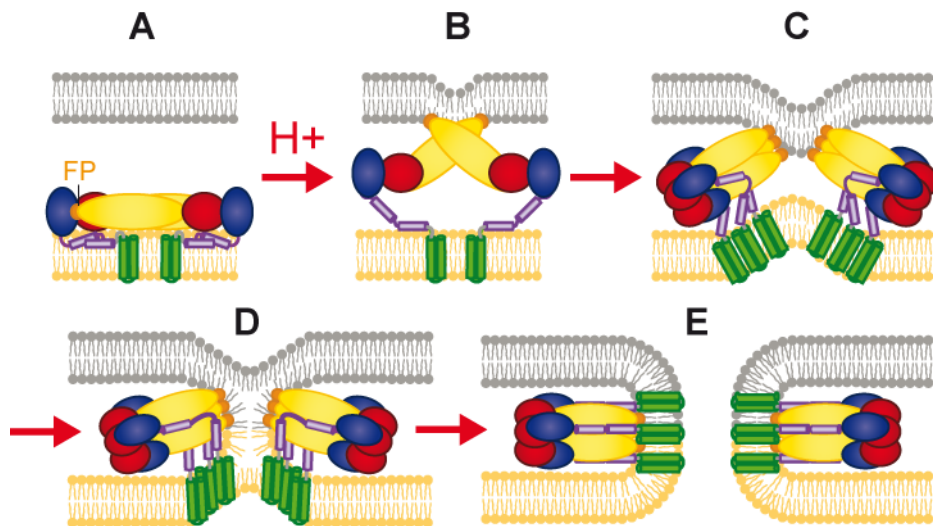


Figure 9: Proposed flavivirus fusion model

(A) Side view of a metastable E homodimer at the surface of a mature flavivirus particle at neutral pH.

(B) Acidic-pH-induced dissociation of the E homodimer and exposure of the FPs. The FPs are able to interact with the target membrane.

(C-D) E trimerization, DIII relocation and the zippering of the stem along the E trimer.

(D) Generation of a hemifusion intermediate in which only the outer leaflets of the host and viral membranes are fused.

(E) Formation of the E protein post-fusion structure and opening of a fusion pore.

Color code for the E protein as described in Figure 3; target membrane, grey; viral membrane, orange.

Figure adapted from (Fritz, Blazevic et al. 2011).

2.4.2.3 DI-DIII interface of the E protein

In the metastable pre-fusion E protein, the fusion peptide at the tip of DII is buried at the DI/DIII interface of the second monomer (Stiasny and Heinz 2006) (Figure 10). There are two conserved histidines (H146, and H323) and one conserved salt bridge (E373-R9) which are important for stabilizing this interface (Bressanelli, Stiasny et al. 2004; Kampmann, Mueller et al. 2006; Fritz, Stiasny et al. 2008). The destabilization of these contact residues is necessary for the release of the FP, as well as the relocation of DIII during the conformational changes of E and thus for the entire fusion process (Bressanelli, Stiasny et al. 2004).

Since the pH threshold of flavivirus membrane fusion is around 6.6 (Gollins and Porterfield 1986; Corver, Ortiz et al. 2000; Moesker, Rodenhuis-Zybert et al. 2010) and the pKa of histidine is between 6 and 7, histidine residues have been proposed to act as low-pH sensor (Bressanelli, Stiasny et al. 2004; Stevens, Corper et al. 2004; Kampmann, Mueller et al. 2006; Kanai, Kar et al. 2006; Roussel, Lescar et al. 2006; Mueller, Kampmann et al. 2008; Roche, Albertini et al. 2008; Qin, Zheng et al. 2009). At neutral pH, histidine (H) residues are uncharged and become protonated and positively charged at the acidic pH in the endosomes.

The 5 histidine residues conserved among all flavivirus proteins E (H146, H248, H287, H323 and H438 in TBEV) were analyzed with mutated RSPs of TBEV E (Fritz, Stiasny et al. 2008) (Figure 10). Two of these residues are located at the domain I/III interface (H146 and H323), H248 is located in DII, H287 in DI and H438 in the stem. Single substitutions of H248, H287 and H438 had no effect on fusion, but replacing H323 by alanine (H323A) led to a dramatic reduction of fusion activity with liposomes (Fritz, Stiasny et al. 2008). Further investigations identified that early steps of membrane fusion (dissociation of the protein E dimer, FP exposure and initial membrane interactions) were impaired in the H323A mutant. In this study it was not possible to investigate the role of H146 because its mutation abolished RSP production (Fritz, Stiasny et al. 2008).

A study using the flavivirus system of WN and Langkat virus demonstrated that histidine mutants (corresponding to H146 and H323 of TBEV) still produced infectious virions (Nelson, Poddar et al. 2009), but neither fusion activities nor specific infectivities of these mutants have been determined in this study.

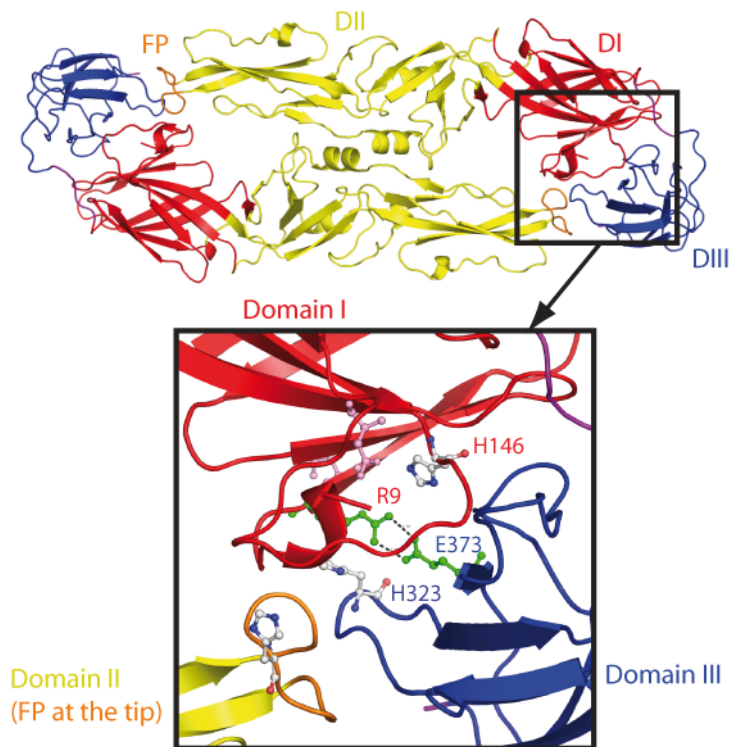


Figure 10: Intramolecular interactions at the DI/DIII interface

Ribbon diagram of the TBEV sE dimer and the details of the interface between DI and DIII in the pre-fusion conformation. H146, H323 and the salt bridge between E373 and R9 are highlighted.

2.4.2.4 Stem-anchor region of the E protein

Although the crystal structure of soluble E proteins lack the stem-anchor region, improved techniques for reconstructing cryo-electronmicroscopy images made it possible to determine these regions in the native conformation (Zhang, Chipman et al. 2003). In the pre-fusion protein E, the two amphipathic helices of the stem lie flat on the viral membrane and are partially buried in the outer lipid leaflet by hydrophobic interactions while the TM anchor form an antiparallel hairpin structure (Zhang, Chipman et al. 2003).

Although no structural details are available for the stem-anchor region in the post-fusion trimer, the orientation of the C-terminus of sE in its post-fusion conformation and modeling studies, however, indicate that the stem follows a groove between the domains II alongside the body of the trimer (Bressanelli, Stiasny et al. 2004). The high hydrophobicity of the stretch of amino acids N-terminal to the TM domains could be involved in interactions with the FPs and/or membranes during fusion.

Biochemical studies implicated that the stem acts as a stabilizing feature for the post-fusion trimer (Stiasny, Kossl et al. 2005). In the absence of target membranes, the stem helix 1 was essential for trimerization of the E protein (Allison, Stiasny et al. 1999).

The E protein is the only known viral fusion protein carrying a double membrane anchor which is composed of two antiparallel transmembrane helices (TM1 and TM2) with different functions in polyprotein processing. TM1 acts as a stop-transfer sequence and TM2 as an internal signal sequence for the translocation of the first non-structural protein into the lumen of the ER (Lindenbach 2007).

All other fusion proteins (class I, III and the class II of alphaviruses) have a single transmembrane domain. These transmembrane domains anchor the proteins in the viral membrane and are followed by a cytoplasmic tail of varying lengths (White, Delos et al. 2008).

The unique organization of the C-terminal part of flavivirus fusion protein E has not been ascribed a specific functional role in the fusion mechanism. Using the TBEV RSP model system Fritz and colleagues addressed the question whether the double membrane anchor of the E protein is necessary for flavivirus membrane fusion or is merely a remnant of polyprotein processing. TM2 helix was shown to be completely dispensable for the early steps of membrane fusion, but was required for E trimer stability and efficient fusion. The data in this study provided evidence, that both intra- and inter-trimeric interactions mediated by the TM helices of E are involved in flavivirus membrane fusion (Fritz, Blazevic et al. 2011).

3 Objectives

The overall goal of this diploma thesis was the generation and characterization of TBEV protein E mutants that allow the investigation of the flavivirus fusion process in more detail. Specifically, two aspects were investigated in an infectious system: the functional role of 1. the E protein membrane anchor and 2. conserved residues at the DI/DIII interface of the E protein.

3.1 Analysis of the functional relevance of the transmembrane hairpin of flavivirus in membrane fusion

The flavivirus envelope protein E is the only known viral fusion protein with a double membrane anchor, consisting of two antiparallel transmembrane helices (TM1 and TM2) (Figure 2 and 4). The possible role of this peculiar hairpin in membrane fusion has been addressed by studying TM mutants of tick-borne encephalitis virus (TBEV) recombinant subviral particles (RSPs). The membrane anchor of E was modified by deleting the TM2 helix, replacing both TM domains by those of a heterologous flavivirus (Japanese encephalitis virus, JEV), and shuffling the TM domains between TBEV and JEV. Functional analysis of these mutant RSPs demonstrated that the TM2 helix was completely dispensable for the early steps of membrane fusion but essential for later steps. The data obtained with RSPs not only provided evidence for a role of the TM helices in intra-trimer interactions but also indicated their participation in inter-trimer interactions that are both necessary for efficient fusion.

To assess the significance of the observations made with RSP TM mutants in the context of infectious virions, heterologous and chimeric membrane anchors (JE TM1-JE TM2, TBE TM1-JE TM2, and JE TM1-TBE TM2) were engineered into an infectious cDNA clone of TBEV for this thesis. The obtained virus mutants were characterized with respect to their infectious properties. Since the TM2 element is indispensable for polyprotein translation and thus for the generation of infectious virions, a Δ TM2 mutant could not be analyzed.

3.2 Investigation of key residues of the E protein involved in triggering membrane fusion

Using RSPs of TBEV, the mutational analysis of histidines conserved among all flavivirus E proteins provided evidence that H323 is an important residue in the initiation of the low-pH-dependent multistep fusion process. H323 is located at the domain I/III interface which contains a network of interactions between the two domains within one E monomer and a salt bridge between R9 (domain I, DI) and E373 (domain III, DIII). The destabilization of the DI/DIII interface by protonation is essential for the structural changes of protein E and thus for the entire fusion process.

In contrast to these results, the substitutions of histidines – in the context of single round infectious particles of West Nile and Langat virus – still allowed pH-dependent infection of cells. Some of the identified mutants were less infectious than wild type, but specific infectivities were not determined and the effect of these mutations on fusion was not investigated.

Further experiments – both in vitro fusion experiments and standardized infectivity assays – are needed to clarify this issue. Therefore – as the second part of the thesis – the two conserved histidines at the DI/DIII interface (H146 which could not be analyzed in the context of RSPs, H323) and E373 were mutated in the infectious cDNA clone of TBEV. The obtained virus mutants were then characterized with respect to their infectious properties.

4 Materials and Methods

4.1 Materials

4.1.1 Cells

Baby hamster kidney cells - BHK-21 cells (ATCC no. CCL-10™) - were grown in Eagle's minimum essential medium (Sigma-Aldrich) containing 5% fetal calf serum (FCS), 1% glutamine, and 0.5% neomycine (growth medium) at 37°C and 5% CO₂. The maintenance medium for BHK-21 cells was composed of Eagle's minimum essential medium (Sigma-Aldrich) containing 1% fetal calf serum (FCS), 1% glutamine, 0.5% neomycine, and 15 mM HEPES, pH 7.4.

4.1.2 Viruses

In all experiments, the European subtype TBEV strain Neudoerfl (Mandl, Heinz et al. 1988; Mandl, Heinz et al. 1989) (GenBank accession no. U27495) was used.

For the cloning of TMD mutants the Japanese encephalitis (JE) virus strain Nakayama (GenBank accession no. EF571853) was used.

4.1.3 Plasmids

The pTNd/c plasmid contains the complete genomic cDNA of the TBE virus strain Neudoerfl (sequence 1- 11141 Nt) inserted into the vector pBR322 under the control of a T7 transcription promoter (Mandl, Ecker et al. 1997).

The pTNd/5' plasmid contains the 5' terminal one third of TBE virus strain Neudoerfl cDNA (sequence 1-3155 Nt) inserted into the vector pBR322 under the control of a T7 transcription promoter (Mandl, Ecker et al. 1997).

4.2 Methods

4.2.1 Cloning of transmembrane hairpin mutants

Full-length cDNA clones containing modified E membrane anchors were generated by the substitution of the original anchor region with chemically synthesized DNA fragments (GeneArt). The synthesized constructs consisted of heterologous membrane anchor of JEV (JE1-JE2) or shuffled membrane anchors (JE1-TBE2, TBE1-JE2). These synthesized DNA fragments were first amplified and then introduced into the full-length cDNA clone pTNd/c by taking advantage of unique restriction sites (SnaBI nucleotide (nt) position 1880 and ClaI nt position 3155).

4.2.2 Cloning of DI/DIII interface mutants

Mutations at the codon positions 146, 323, or 373 of the E protein gene were first introduced into the pTNd/5' plasmid using the site-directed mutagenesis kit Gene Tailor (Invitrogen). The sequences of the primers (VBC Biotech) used for the mutagenesis PCR are listed in Table 1.

Table 1: Oligonucleotide primers for mutagenesis PCR

Primer	Orientation	Sequence (5' to 3')	Position
H146A	sense	CG GTC AAA GTC GAA CCA GCG ACG GGA GAC T	1391-1420
H146N	sense	CG GTC AAA GTC GAA CCA AAC ACG GGA GAC T	1391-1420
H146 rev	antisense	TGG TTC GAC TTT GAC CGT GTA CAC TAT TTT	1378-1407
H323A	sense	GA GCT CCA ACA GAC AGT GGG GCA GAT A	1919-1945
H323A rev	antisense	CCC ACT GTC TGT TGG AGC TCT CTT CCA TG	1910-1938
E373A	sense	GGA GGT GGC TTC ATA GCT ATG CAG CTG CC	2047-2103
E373N	sense	GGA GGT GGC TTC ATA AAT ATG CAG CTG CC	2047-2103
E373 rev	antisense	TAT GAA GCC ACC TCC ATT GTT TTC AAT TGT	2059-2088

Bold letters indicate mutated nucleotides.

Position numbers of matching nucleotides corresponding to the wild type virus genome sequence of TBEV Neudoerfl strain (GenBank accession no. U27495).

These substitutions were then transferred into the full-length cDNA clone pTNd/c (Mandl, Ecker et al. 1997) by taking advantage of two unique restriction sites. For the full-length cDNA clones containing a mutation at codon position 146 of the E protein the restriction enzymes Sall (site located upstream of the TBE virus 5' end) and SnaBI (nt position 1880) were used. The full-length cDNA clones with mutations at codon position 323 and 373 of the E protein were generated by cleavage with SnaBI (nt position 1880) and ClaI (nt position 3155).

For the generation of the H146A-H323A full-length clone, the pTNd/5' fragment carrying H146A mutation was cloned by cleavage with SnaBI and ClaI into the pTNd/c clone containing the H323A mutation.

All plasmids were amplified in *E. coli* strain HB101 and purified using commercially available systems (Qiagen) according to manufacturer's protocols.

Table 2: Restriction enzymes for generation of full-length cDNA clones.

Mutation	restriction enzymes
H146A	Sall and SnaBI
H146N	Sall and SnaBI
H323A	SnaBI and ClaI
H146A-H323A	SnaBI and ClaI
E373A	SnaBI and ClaI
E373N	SnaBI and ClaI

4.2.3 Agarose gel electrophoresis

Separation of DNA fragments was performed by agarose gel electrophoresis. 5x DNA loading buffer was added to DNA samples and loaded on a 1% (wt/v) agarose gel. For size determination of DNA fragments, length marker λ phage DNA digested with HindIII was used. Separation of DNA fragments according to their size was performed by application of a constant voltage of 110 V for 30-40 minutes. The agarose gel contained ethidium bromide (2.5 $\mu\text{g/ml}$) to visualize the DNA fragments under ultraviolet light (320 nm).

4.2.4 DNA sequencing

Sequence analysis of DNA fragments was performed using the Big Dye Terminator Cycle Sequencing Kit from Applied Biosystems according to the manufacturer's instructions. The sequence reaction was carried out in a thermal cycler (Perkin Elmer) using the following program:

	initiation	denaturation	annealing	extension	hold
temperature	96°C	96°C	50°C	60°C	4°C
time	20 sec	30 sec	15 sec	4 min	hold
cycle	1 cycle		35 cycles		1 cycle

Amplified DNA products were purified by centrifugation through swelled Sephadex. The sequence of the DNA samples were analysed with an automatic capillary sequencer (Applied Biosystems, GA 3100) by employing fluorescence-labeled dideoxynucleotides as described in (Sanger, Nicklen et al. 1977). Analysed sequences were aligned using the software DNASTar (DNASTar, Inc.).

4.2.5 In vitro RNA transcription

In vitro transcription of engineered genomic full-length RNA was performed with the T7 RNA polymerase kit (T7 MEGAscript transcription kit from Ambion) as reported previously (Mandl, Ecker et al. 1997; Kofler, Heinz et al. 2002; Elshuber, Allison et al. 2003). The template DNA was degraded by incubation with DNaseI for 15 minutes at 37°C, and the RNA was purified using an RNeasy Mini kit (Qiagen). The correct length and integrity of the synthesized RNA was verified by staining with radiant red and checked on a formalin-denaturing 1% agarose gel. RNA concentration was quantified by spectrophotometric measurement (Mandl, Ecker et al. 1997; Taucher, Berger et al. 2010).

4.2.6 Transfection of BHK-21 cells by electroporation

A subconfluent monolayer of BHK-21 cells grown in a 175 cm² tissue flask was transfected with equal amounts of viral full-length RNA as described previously (Mandl, Ecker et al. 1997). In brief, BHK-21 cell aliquots resuspended in ice-cold PBS were electroporated with in vitro transcribed RNA (7.8 µg). The electroporation was performed by two pulses using a Bio-Rad Gene Pulser (settings: 1.8 kV; 25 µF, 200 Ω) resulting in an optimal time constant of 0.8 milliseconds. The electroporated cells were seeded into a 80 cm² tissue flask containing 10 ml growth medium. The growth medium was replaced about 6 hours post transfection and the concentration of FCS was reduced to 1%.

Cell culture supernatants were harvested 48 hours post-transfection and the supernatants were cleared from cell debris and insoluble material by centrifugation at 10,000 rpm for 20 minutes and 4°C (Beckman JA 14 rotor). The clarified cell culture supernatant, containing the recombinant virions, was stored at -80°C and used for further analysis.

4.2.7 Infection of BHK-21 cells

BHK-21 cells were seeded into 24-well plates (10⁵ cells/well) containing glass cover slips and maintained overnight with growth medium. The growth medium was replaced, the cells were washed three times with minimal medium and 200 µl cell culture supernatant harvested after transfection or infection was added. After incubation for 45 minutes at 37°C and 5% CO₂ the supernatant was removed and the cells were washed two times with minimal medium. 1 ml fresh minimal medium was added and incubated for 48-72 hours.

The cell culture supernatants were harvested and cleared from cell debris and insoluble material by centrifugation at 10,000 rpm for 20 minutes at 4°C (Eppendorf, 5417R). The clarified cell culture supernatant, containing the virions, was stored at -80°C and used for further analysis or infections.

4.2.8 Viral RNA isolation from supernatant and cDNA synthesis

Supernatants derived from transfected and/or infected cells were incubated with 0.5% SDS, 0.8 µg proteinase K (Roche), 40 U RNase inhibitor (Boehringer Mannheim), 4 nM Tris (pH 8.0) and 2 nM EDTA (pH 8.0) for 1 hour at 37°C. To isolate and purify viral RNA, phenol/chloroform extraction and ethanol precipitation were performed (Kandolf and Hofschneider 1985). Viral RNA was transcribed into cDNA by a commercially available kit (cDNA Synthesis Kit, Roche). The transcribed viral cDNA was extracted by phenol/chloroform purification and ethanol precipitation.

4.2.9 Immunofluorescence staining

Transfected or infected BHK-21 cells were grown on glass cover slips. 24 hours post transfection or infection the cells were fixed with acetone/methanol (1:1) for 10 minutes at -20°C, air-dried and washed with phosphate-buffered saline (PBS). The cell monolayer was then incubated with a polyclonal rabbit anti-TBEV serum for 1 hour in a humid chamber at 37°C. After washing with PBS, a fluorescein isothiocyanate-conjugated goat anti-rabbit IgG (H+L) (Jackson immune research laboratory) was added for 45 minutes in a humid chamber at 37°C. Finally, the second antibody was removed, dried and embedded in DePeX (Serva) on microscope slides. Visual inspection was performed with the Microphot-SA microscope from Nikon.

4.2.10 Quantitative TBEV protein E four-layer ELISA

MaxiSorp microtiter plates (96 well, Nunc) were coated with 50 µl polyclonal guinea pig anti-TBEV immunoglobulin (2.5 µg/ml, carbonate buffer pH 9.6) for 48 hours at 4°C. The samples and the protein standard were denatured with sodium dodecyl sulfate (SDS) for 30 minutes at 65°C. Serial dilutions of the denatured samples and standard in ELISA buffer (PBS pH 7.4, with 2% Tween and 2% sheep serum) were transferred to the coated plates and incubated for 2 hours at 37°C in a humid chamber. After washing the plates four times with washing buffer (PBS pH 7.4 with 0.025% Tween) a polyclonal rabbit-anti TBEV serum was added, incubated for 1 hour at 37°C and then washed again. An anti-rabbit IgG peroxidase conjugate from donkey (Amersham) was used to visualize the amount of bound antigen by a reaction with the substrate ortho-phenyldiamine (Sigma-Aldrich). The reaction was stopped after 30 minutes by the addition of 2 N H₂SO₄. The absorbance was measured with a photometer (ELX 808) at the dual-wavelength 490/630 nm using the KC Junior data analysis software (both from BioTek) (Heinz, Stiasny et al. 1994).

4.2.11 Rate zonal gradient centrifugation of viral particles

Virus samples containing equal amounts of protein E were applied to 5-30% (wt/wt) continuous sucrose gradients in TAN buffer pH 8.0 (50 mM TEA, 100 mM NaCl). After centrifugation for 70 minutes at 38,000 rpm and 4°C (Beckman SW 40 rotor), fractions were collected by upward displacement with the BioComp Piston Gradient Fractionator (settings: speed 0.4, distance 4.0 and fraction 20). The E protein concentration in each fraction was quantified by an E protein specific four-layer SDS ELISA (4.2.10).

4.2.12 RNA quantification by real-time PCR analysis

Isolation of viral RNA from the cell culture supernatant harvested 48 hours post transfection was performed using the RNeasy Mini Kit from Qiagen. Reverse transcription of isolated viral RNA was carried out with the iScript cDNA Synthesis Kit from Bio-Rad. The temperature profile of the reaction was: 5 minutes at 25°C, 30 minutes at 42°C, and 5 minutes at 85°C, followed by a hold at 4°C. An aliquote of the cDNA preparation was used for the quantification of viral RNA equivalents by real-time PCR. The TaqMan Universal PCR Mastermix (PE Applied Biosystems) and primers specific for part of the TBEV NS5 coding region were used for the real-time qPCR. Amplification and detection was performed using the ABI 7300 Real Time RCP System (PE Applied Biosystems).

	Initiation 1	Initiation 2	denaturation	annealing	extension
temperature	50°C	95°C	95°C	55°C	72°C
time	3 min	10 min	15 sec	30 sec	31 sec
cycle	1 cycle	1 cycle		45 cycles	

RNA was quantified using a standard curve prepared from a ten-fold dilution series of spectrophotometrically quantified, purified, in vitro-synthesized genomic full-length RNA (Kofler, Hoenninger et al. 2006; Schrauf, Schlick et al. 2008).

4.2.13 Focus formation assay

BHK-21 cells were seeded into 24-well plates (10^5 cells/well) and cultured in growth medium for 24 hours followed by washing with maintenance medium. Ten-fold serial dilutions of infectious supernatants were transferred to these cell monolayers and incubated for 4 hours at 37°C and 5% CO₂. The supernatant was removed and 1 ml 3% carboxymethyl cellulose (CMC) in maintenance medium was added. The cells were further incubated for two days at 37°C and 5% CO₂. The CMC overlay was removed, the cells were washed three times with PBS (pH 7.4), fixed and permeabilised with acetone/methanol (1:1) for 10 minutes at -20°C. The fixed cells were blocked with PBS containing 5% sheep serum for 30 minutes at RT and incubated with polyclonal rabbit-anti TBEV serum in PBS (pH 7.4 with 0.2% Tween and 3% sheep serum) for 1 hour at 37°C. Antibody-labeled cells were detected with an anti-rabbit IgG alkaline phosphatase conjugate (Sigma-Aldrich) in TBS buffer (0.2% Tween and 3% sheep serum) and Sigma Fast Red TR/naphthol AS-MX as a substrate. The reaction was stopped with ddH₂O and the formed foci were counted.

5 Results

5.1 Analysis of the functional relevance of the transmembrane hairpin of flavivirus in membrane fusion

The flavivirus E protein is the only known fusion protein with a membrane anchor consisting of two transmembrane helices (TM1, TM2). Using RSPs with truncated (lacking TM2) and chimeric forms of the E protein (containing heterologous flavivirus TM segments) it was shown that both TM helices are crucial for efficient fusion (Fritz, Blazevic et al. 2011). TM interactions apparently contribute to the stability of the post-fusion trimer and the completion of the merger of the membranes.

The goal of this diploma thesis was to assess the significance of the observations made with TBEV RSP TM mutants also in the context of infectious virions. Therefore chimeric E membrane anchors were cloned into an infectious cDNA clone of TBEV to characterize the resulting virions. Since the TM2 element is indispensable for polyprotein translation and thus for the generation of infectious virions (see section 2.2.1), a mutant lacking TM2 could not be analyzed in this study.

5.1.1 Generation of full-length cDNA clones

To investigate the role of TM domain modifications of the E protein in the infectious system, the following TBEV constructs were generated: 1. replacement of the complete TM hairpin by the heterologous TM hairpin of JEV, a distantly related flavivirus (JE1-JE2), 2. generation of a chimeric hairpin in which the TM2 domain was replaced by that of JEV (TBE1-JE2) and 3. generation of a chimeric hairpin in which the TM1 domain was replaced by that of JEV (JE1-TBE2) (Figure 11A). Fragments containing the desired heterologous TMD sequences (synthesized by Genart, amino acid sequences shown in Figure 11B) were cloned into the backbone of the full-length cDNA virus genome plasmid pTNd/c (Mandl, Ecker et al. 1997) as described in Materials and Methods. Successful cloning was confirmed by verification of the correct size of the plasmid by agarose gel electrophoresis (Figure 12) and sequence analysis. Two bands were detected in the agarose gel that corresponded to different forms of the plasmid. The band at 14,802 bp most likely represented the linear form of the plasmid while the upper band corresponded to the nicked circle form. These two bands indicated the correct size of the engineered plasmids. Sequencing the final full-length cDNA clones revealed that they contained only the desired anchor modifications, but no additional mutations.

5.1.2 Characterization of mutant viruses

5.1.2.1 Production of mutant viruses

To obtain recombinant viruses, mutated and wt full-length cDNA clones were transcribed *in vitro* into RNA. After transfection of BHK-21 cells with the corresponding RNA, cells were seeded into cell culture flasks and the cell culture supernatants were harvested 48 hours after transfection as described in Materials and Methods.

To verify the sequences of the virus in the supernatant after primary transfection, viral RNA was isolated and used for cDNA transcription. The region coding for the structural proteins as well as the first 40% of NS1 were sequenced. In all cases, the sequences contained the desired modifications without additional mutations.

To proof that replication and translation have occurred, immunofluorescence staining of transfected cells was performed. In brief, BHK-21 cells transfected with viral RNA were fixed and stained 24 hours post transfection as described in Materials and Methods. As shown in Figure 13A, no differences were observed between wt and mutant-transfected cells.

5.1.2.2 Infectious properties of mutant viruses

To determine whether transfected cells released infectious virus particles, the cell culture supernatants of the experiments displayed in Figure 13A, were harvested 48 hours post transfection and transferred to fresh cells. Immunofluorescence staining of infected cells was performed after 24 hours. Only few positive cells were detected in the case of the mutants in contrast to the wt control (Figure 13B), indicating that mutated virions were significantly reduced in infectivity compared to TBEV wt.

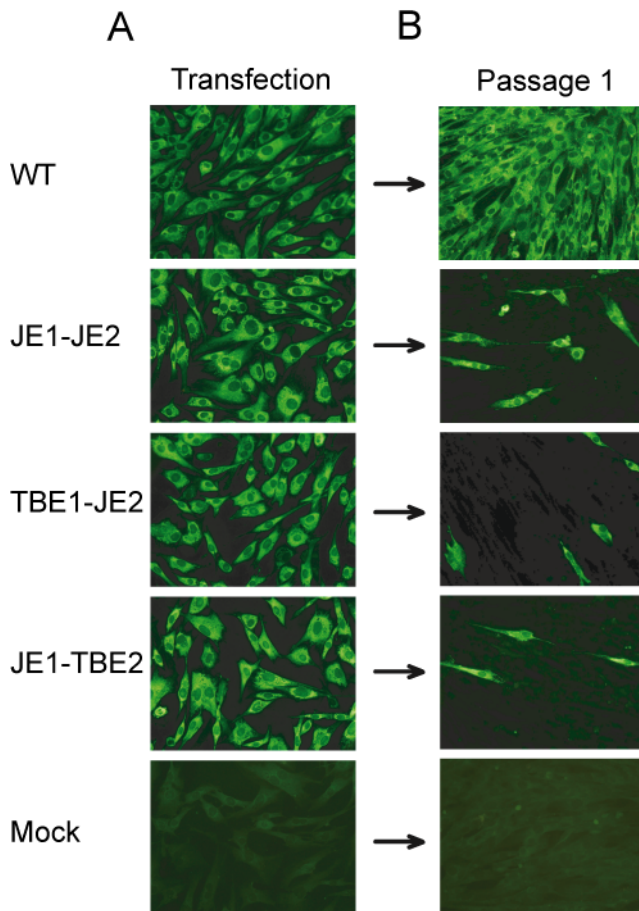


Figure 13: Immunofluorescence staining of (A) transfected and (B) infected BHK-21 cells

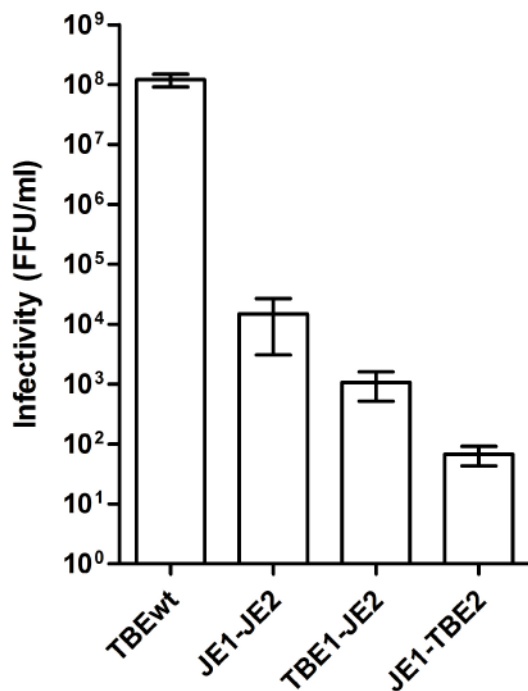
(A) Immunofluorescence staining of BHK-21 cells transfected with either mutant or wt viral RNA is indicated in the left panels. (B) Immunofluorescence staining of cells infected with cell culture supernatants harvested 48 hours after transfection. Staining was performed using a polyclonal serum recognizing the structural proteins of TBEV. At least two independent experiments were carried out. Immunofluorescence pictures from one representative electroporation are shown.

To quantify the infectivity of cell culture supernatants harvested 48 hours post transfection, focus formation assays were carried out. The infectious titers of the mutants viruses were at least ~10,000-fold lower than that of the wt control (Figure

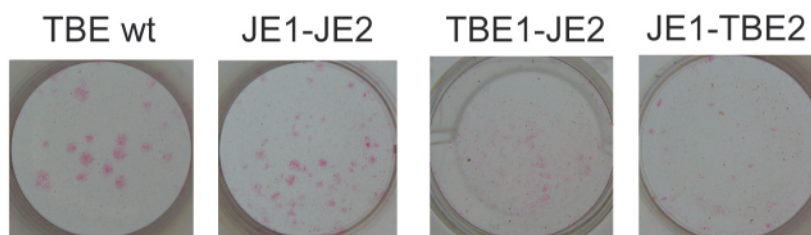
14A). Inspection of the foci revealed a reduced size for the mutants compared to wt, especially for mutants TBE1-JE2 and JE1-TBE2 (Figure

14B). Taken together, the introduced modifications had a significant influence on the infectivity of mutants.

A



B

**Figure****14: Infectivity of E protein TMD mutations in BHK-21 cells**

(A) Quantification of virus in cell culture supernatants harvested 48 hours after transfection (Figure 13B) by focus formation assays. Two independent experiments were carried out in duplicates. The data represent the means of these two experiments and the error bars indicate the observed range. Focus forming units (FFU).

(B) Focus morphology of wild type and mutant viruses.

To investigate the specific infectivity of cell culture supernatants harvested 48 hours post transfection, the ratio of RNA equivalents to infectious units was determined. For that purpose, viral RNA molecules released into the cell culture supernatant were quantified using quantitative real-time PCR as described in Materials and Methods. Analysis of RNA equivalents in the cell culture supernatant revealed that also the specific infectivities of the mutant viruses were reduced compared to the wt.

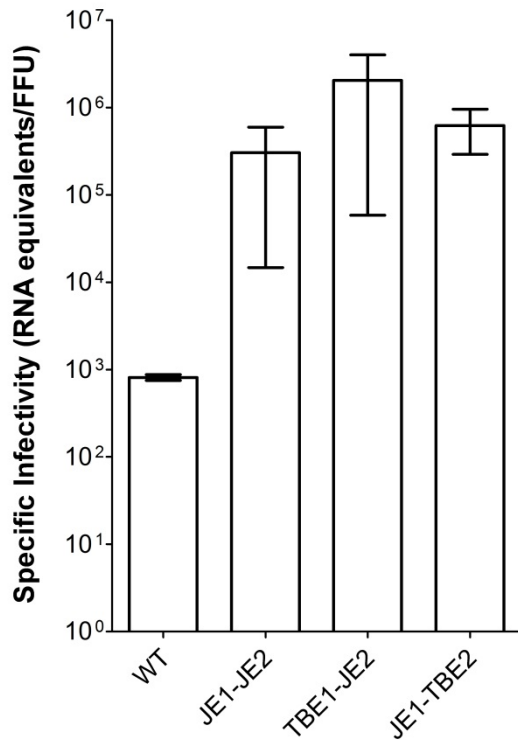


Figure 15: Specific Infectivity of E protein TMD mutations

Determination of the specific infectivities (RNA equivalents per infectious units) of virus in the cell culture supernatants harvested 48 hours after transfection. Two independent experiments were performed in duplicates. The data represents the means of these two experiments and the error bars indicate the observed range.

5.1.2.3 Expression and characterization of the E protein in the cell culture supernatant of transfected cells

Only low infectivities were observed for the mutant viruses, but it still remained unclear whether less particles were secreted or whether secreted particles were less infectious. Therefore, E secreted into the cell culture supernatant was quantified by an E protein specific four-layer SDS-ELISA and the organization of E (soluble, particulate) was investigated by rate zonal gradient centrifugation. As shown in Figure 16, for two mutants TBE1-JE2 and JE1-TBE2 similar amounts of the E protein were detected in the cell culture supernatants of transfected cells compared to wt. Mutant JE1-JE2 revealed a reduced E protein concentration in the cell culture supernatant of about 35%.

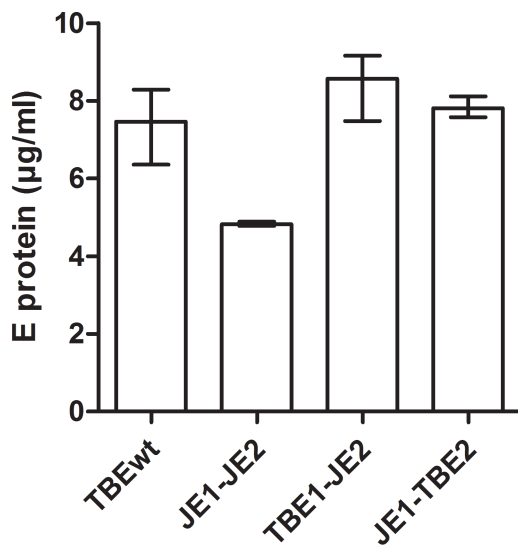


Figure 16: E protein concentrations of cell culture supernatant 48 hours post transfection

Quantification of the E protein concentrations in cell culture supernatants 48 hours post transfection. Mean values of 2 independent ELISA measurements of one representative electroporation are shown, error bars represent observed range.

To find out whether the secreted E protein is incorporated into viral particles, rate zonal gradient centrifugation was performed. Briefly, the supernatants of TBEV wt and mutant viruses were applied on sucrose gradients, centrifuged for 70 minutes and fractionated as described in Materials and Methods. A gradient with purified TBE virus was run in parallel and served as a control.

Dramatic differences in the distribution of the E protein in the gradients were observed (Figure 17). Only in the case of recombinant TBE wt virus, the E protein was detected in the fractions 13-16 corresponding to infectious virions. In the case of mutant viruses, however, the E protein was detected only in the upper fractions which indicated soluble E protein, not integrated into particles.

Taken together, due to the low infectivities and low amounts of virus particles secreted it was not possible to produce sufficient amounts of mutant viruses for biochemical analyses.

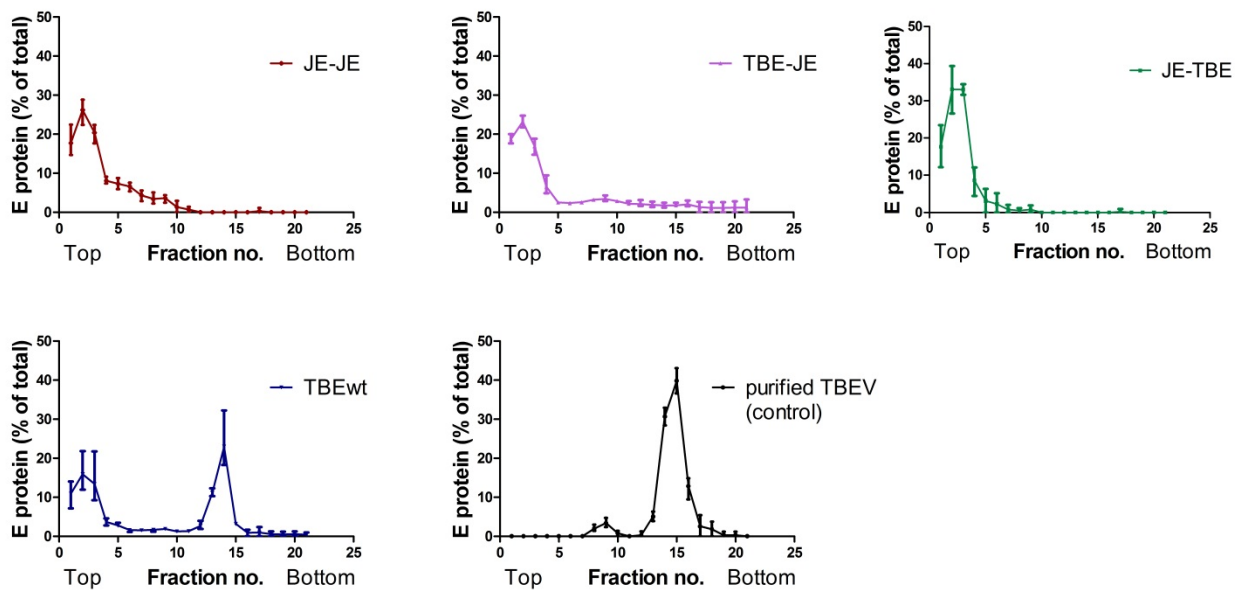


Figure 17: Analysis of particle formation by rate zonal gradient centrifugation

Sedimentation analysis of supernatants from transfected cells with wt and mutant RNAs. The sedimentation direction is from left to right. Results are expressed as percentage of E found in the fractions in relation to the total amount of E in the gradient. The error bars indicate the range of two determinations of E by ELISA.

5.1.2.4 Analysis of resuscitating mutations

To select possible resuscitating mutations and examine mutant virus stability, a total of four serial passages of cell culture supernatants from transfected cells was performed. Cell culture supernatant from the last passage was used for RNA isolation, cDNA synthesis and sequencing of the structural proteins as described in Materials and Methods. This supernatant was also used for the infection of fresh cells (fifth passage) and immunofluorescence staining.

After four serial passages of the infectious supernatant no resuscitating or additional mutations were found. The immunofluorescence staining of infected cells in the fifth passage corresponded to that of the first passage (compared in Figure 18). Taken together, viruses containing the introduced anchor modifications remained stable, during five serial passages.

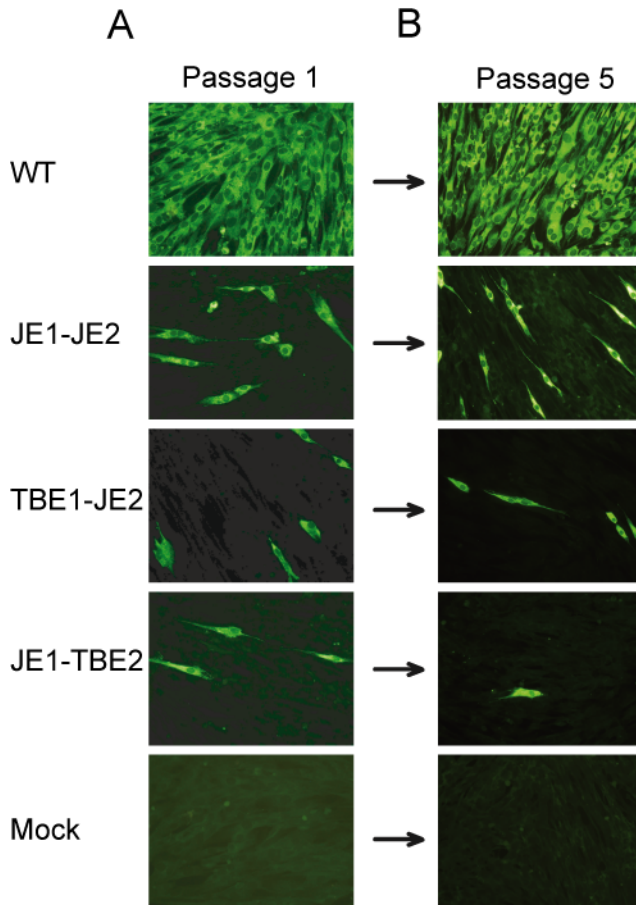


Figure 18: Immunofluorescence staining of BHK-21 cells after (A) first and (B) fifth passage

(A) Immunofluorescence staining of BHK-21 cells infected with the cell culture supernatants harvested 48 hours after transfection. (B) Immunofluorescence staining of BHK-21 cells infected with the supernatants after the fourth passage. Staining was performed using a polyclonal serum recognizing the structural proteins of TBEV. Two independent experiments were carried out. Immunofluorescence pictures from one representative electroporation are shown.

5.2 Investigation of key residues of the E protein involved in triggering membrane fusion

In a previous study, a mutagenesis approach (Figure 19) was utilized to identify the involvement of 5 conserved histidine residues in flavivirus membrane fusion using recombinant subviral particles of TBEV (Fritz, Stiasny et al. 2008). Mutation of H323 was shown to be important for the initiation of fusion whereas that of H146 could not be analyzed in the RSP system because it abolished RSP formation (Fritz, Stiasny et al. 2008).

To study the observations made with RSPs also in the context of infectious virions, amino acid substitutions at position 323 and 146 were introduced in infectious TBEV cDNA clones and the resulting virions were characterized.

5.2.1 Generation of full-length cDNA clones

The used cloning strategy for the generation of mutated full-length cDNA clones is illustrated in Figure 19.

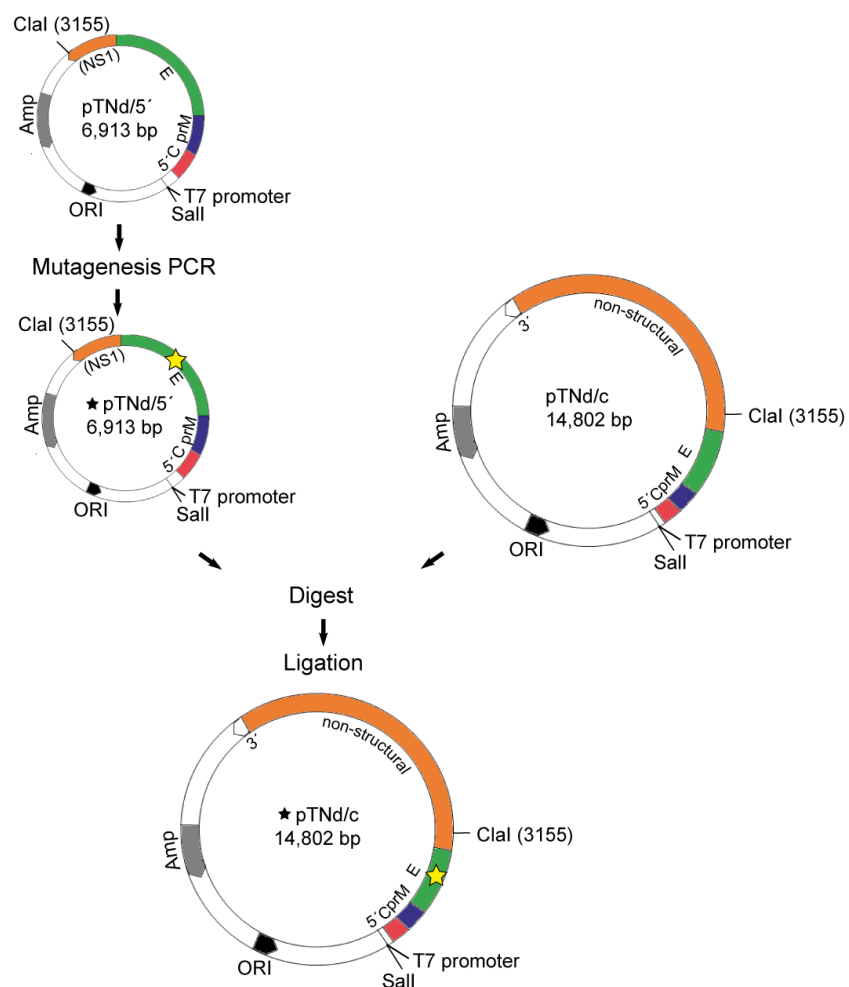


Figure 19: Schematic representation of the cloning strategy

For detail see 5.2.1.1 and 5.2.1.2. Yellow star indicates introduced amino acid substitution.

5.2.1.1 Mutagenesis of pTNd/5' cDNA clones

To test the effect of replacing conserved residues at the DI/DIII interface of the E protein in the infectious system (TBEV), mutations were introduced into the plasmid pTNd/5' (Figure 19), having an insert coding for C, prM, E and partly NS1, by site-directed mutagenesis as described in Materials and Methods. Figure 20 displays the single and combination mutations used in this study: As in the RSP system, H323 was mutated to alanine. H146 was replaced by both, alanine and asparagine. A double mutant, in which both histidines at the DI/DIII interface (146, 323) were substituted by alanine, was also constructed. E373 is highly conserved and located at the DI/DIII interface. Depending on the environment in the protein, glutamate residues could act as alternative pH sensors (Srivastava, Barber et al. 2007). Therefore TBEV protein E was also mutated by replacing E373 by alanine or asparagine, respectively.

Engineered plasmids were transfected in *E. coli* HB101 cells and colonies were picked for plasmid preparation as described in Materials and Methods.

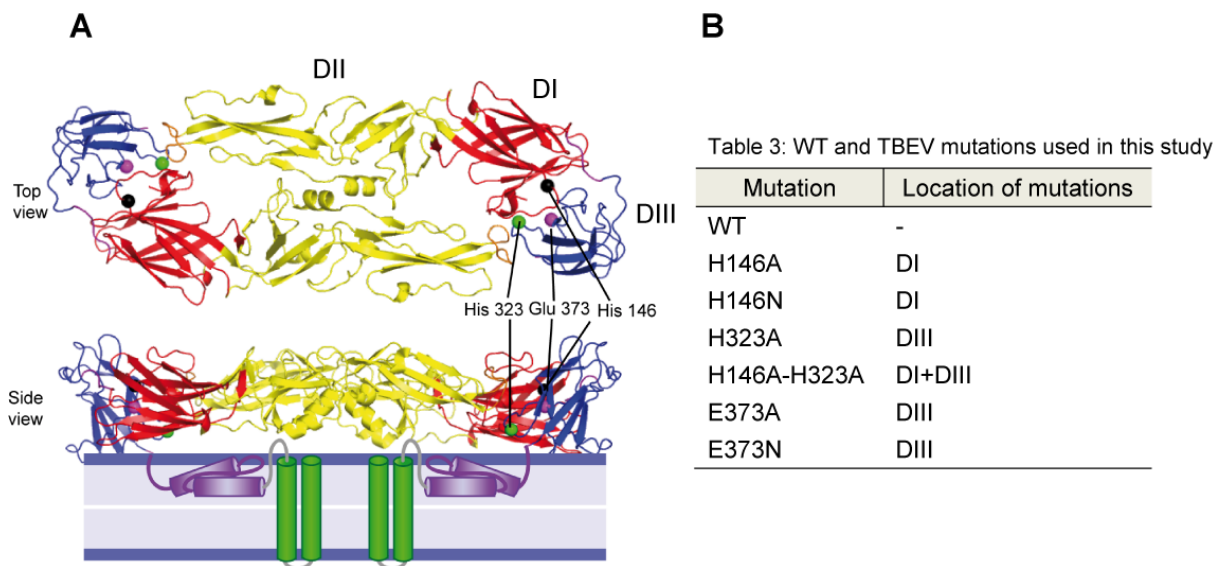


Figure 20: Location of the mutated residues in the E protein

(A) Schematic of the E dimer including ribbon diagrams of sE of TBEV and the stem-anchor region. The residues mutated in this study are indicated by coloured spheres: H146, black; H323, green; E373, pink. Stem-anchor regions for which the atomic structure is unknown are represented schematically. Color code of E as described in Figure 4. (B) Amino acid substitutions and their location in the E protein.

To verify the correct size of the desired plasmid, agarose gel electrophoresis was performed (Figure 21). The appearance of two bands indicated the correct size of the plasmids (6,913 bp). Additionally, the sequence of the designed clones was checked by sequence analysis. Sequence analysis revealed that only the introduced single amino acid mutations were present.

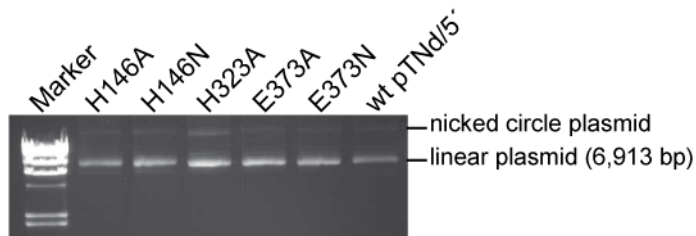


Figure 21: Agarose gel of mutated and wt pTNd/5' cDNA clones

Agarose gel electrophoresis of purified mutant and wt pTNd/5' CDNA plasmids carrying introduced single amino acid substitutions. As a size marker, λ - DNA digested with HindIII was used.

5.2.1.2 Construction of full-length cDNA clones

To generate full-length cDNA clones of TBE virus with the mutations listed in Figure 20B, pTNd/5' was digested with restriction enzymes (shown in Table 2) and cloned into the backbone of the wild type TBEV full-length cDNA clone treated with the same enzymes (Figure 18). Mutated plasmids were transfected into E. coli HB101 and colonies were picked for plasmid preparation as described in Materials and Methods. To confirm successful cloning, agarose gel electrophoresis and sequence analysis was performed. As shown in Figure 22, the presence of two bands indicated the correct size of the plasmids. Sequence analysis of the final full-length cDNA clones revealed no additional mutations except the introduced amino acid substitutions.

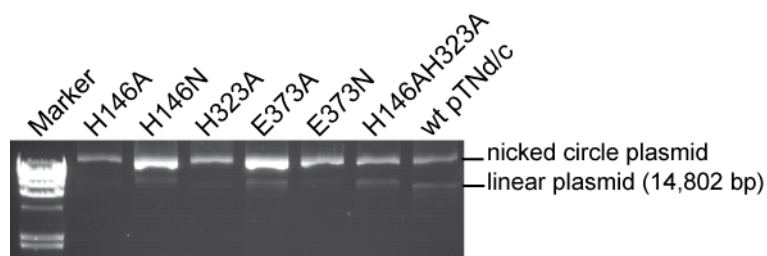


Figure 22: Agarose gel of full-length cDNA clones

Agarose gel electrophoresis of purified mutant and wt full-length cDNA plasmids carrying introduced modifications in the E protein. As a size marker, λ - DNA digested with HindIII was used.

5.2.2 Characterization of mutant viruses

5.2.2.1 Production of mutant viruses

For the generation of recombinant viruses, modified and wt cDNA full-length clones were transcribed in vitro into RNA, and transfected into BHK-21 cells as described in Materials and Methods.

The cell culture supernatants harvested 48 hours after transfection were used for further analysis: First, sequence analysis was performed to verify the sequence of the released virions. Viral RNA was isolated and used for cDNA transcription as described in Materials and Methods. The region coding for the structural proteins as well as the first 40% of NS1 was sequenced. For all mutant viruses, the sequences contained the introduced modifications without additional mutations.

To provide evidence for replication and transfection of the viral genome, indirect immunofluorescence staining of transfected cells was performed. For this purpose, BHK-21 cells transfected with viral mutant or wt RNA were fixed and stained 24 hours post transfection as described in Materials and Methods. Mutant and wt transfected cells did not reveal differences in the immunofluorescence staining (Figure 23A).

5.2.2.2 Infectious properties of mutant viruses

To determine whether transfected cells released infectious particles, the cell culture supernatants obtained 48 hours after transfection were transferred to fresh cells and immunofluorescence staining 24 hours post infection was performed. As shown in Figure 23B, no differences were observed for mutant viruses H146A, H146N and H323A and wt, whereas a reduction was observed with mutant virus H146A-H323A. Mutant virus E373 lost infectivity completely.

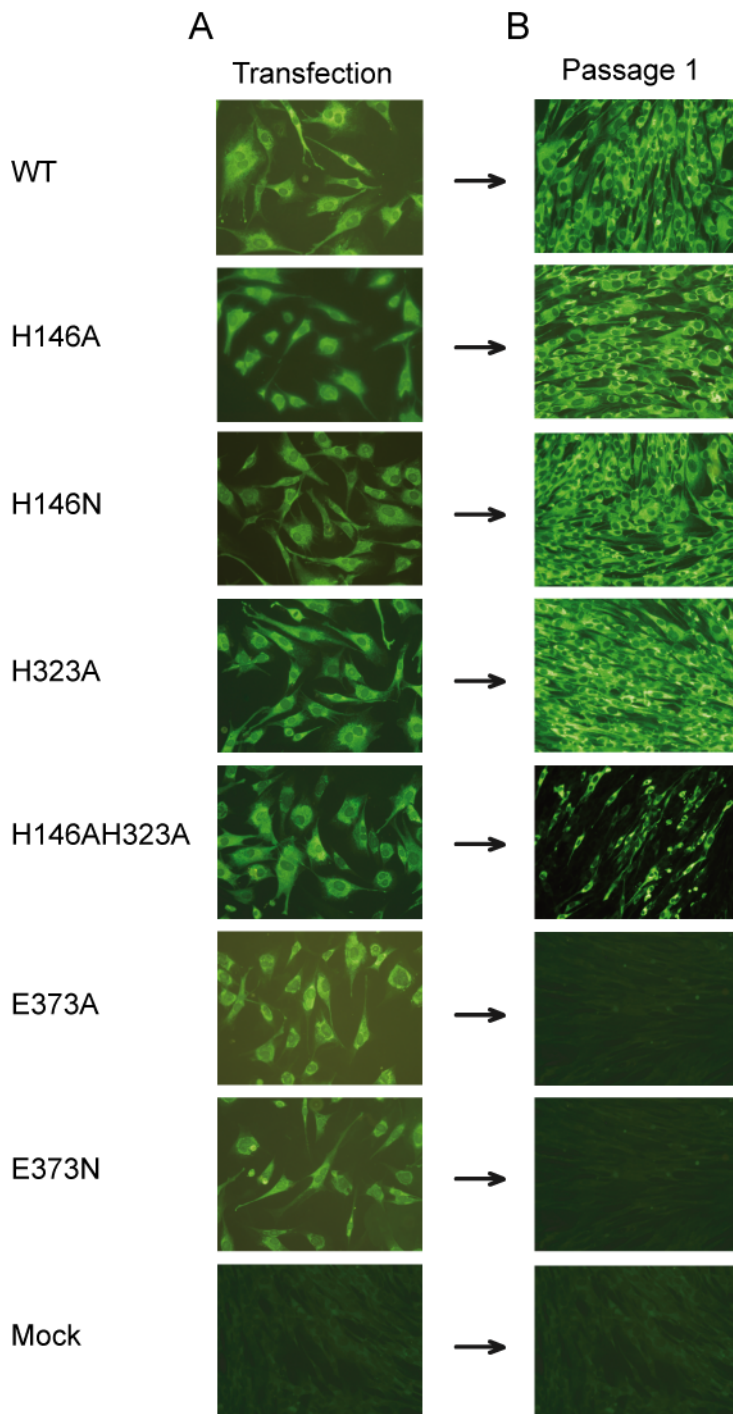


Figure 23: Immunofluorescence staining of (A) transfected and (B) infected BHK-21 cells

(A) Immunofluorescence staining of BHK-21 cells transfected with mutant or viral RNA. (B) Immunofluorescence staining of BHK-21 cells infected with cell culture supernatants harvested 48 hours after transfection. Staining was performed using a polyclonal serum recognizing the structural proteins of TBEV. Immunofluorescence pictures from one representative electroporation are shown.

In order to quantify infectious particles, the cell culture supernatants harvested 48 hours after transfection were analyzed by focus formation assays as described in Materials and Methods. As shown in Figure 24A, mutations H146A, H146N and H323A exhibited a ~10-fold lower infectivity and mutant H146A-H323A a ~100-fold lower infectivity. Consistent with the immunofluorescence data, mutant viruses E373 did not contain infectious particles. H146A and H146A-H323A mutants formed smaller foci compared to wt while the focus size of the other mutants was not affected (Figure 24B).

Taken together, the infectivity of the generated histidine mutants was reduced whereas mutations at position E373 abolished infectivity completely.

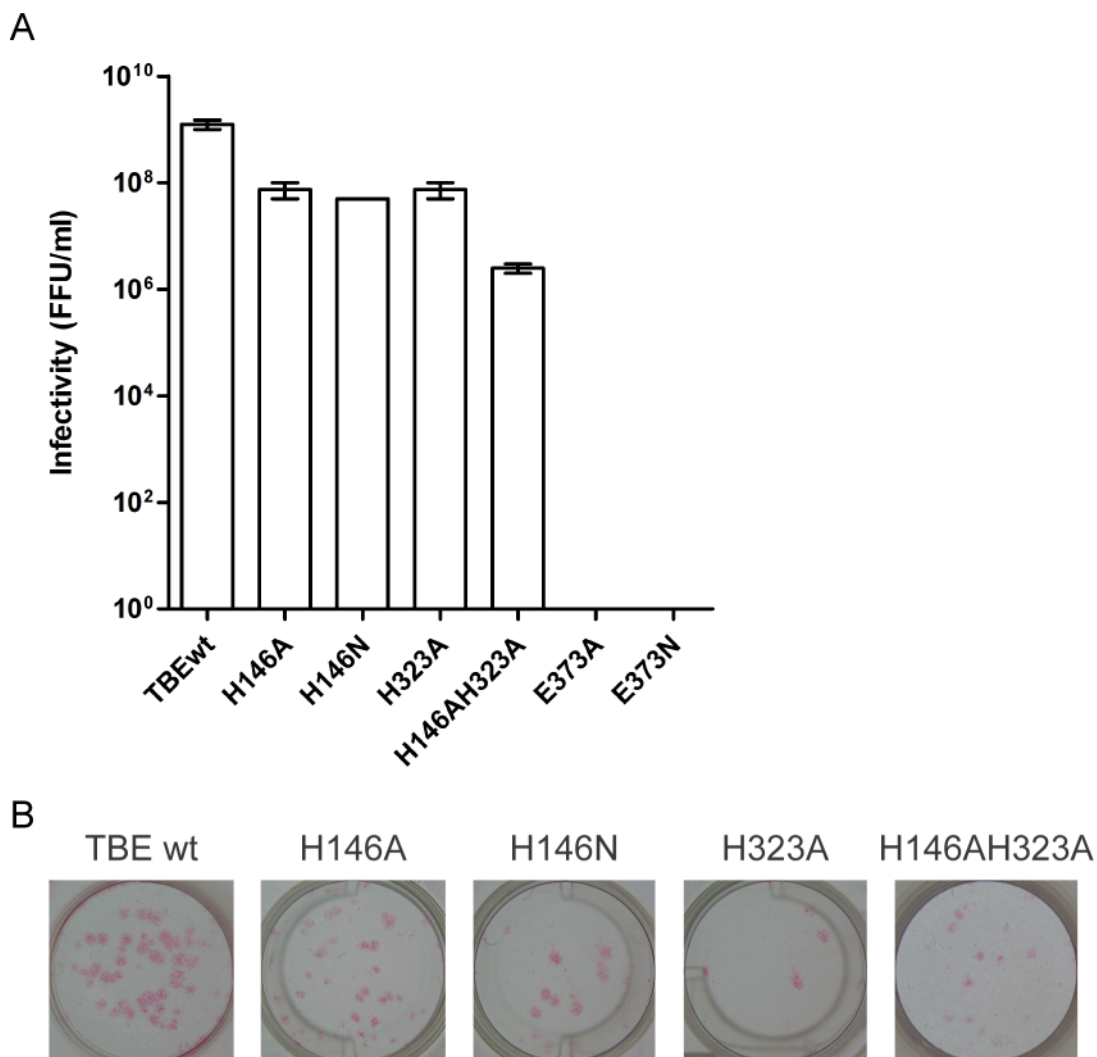


Figure 24: Infectivity titers of E substitutions (DI/DIII interface) in BHK-21 cells

(A) Quantification of virions in cell culture supernatants harvested 48 hours after transfection by focus formation assay. The data represents the means of a representative electroporation carried out in duplicates (error bars represent the observed range). (B) Focus morphology of wild type and mutant viruses.

5.2.2.3 Expression and characterization of the E protein in the cell culture supernatant of transfected cells

Reduced infectivities were observed for the mutant viruses, but it still remained unclear whether less particles were secreted or whether secreted particles were less infectious. Therefore, the E protein secreted into the cell culture supernatants was quantified and the organization of E (soluble, particulate) was investigated by rate zonal gradient centrifugation. In order to find out whether the mutant viruses secrete comparable amounts of E, the cell culture supernatants were quantified in an E specific four-layer ELISA. As shown in Figure 25 mutant viruses – with the exception of E373A – secreted E protein, although the concentration was dramatically lower compared to wt, but the reduction of released E protein (4 to 8-fold) was not as pronounced as reduction in infectivity (10 to 100-fold).

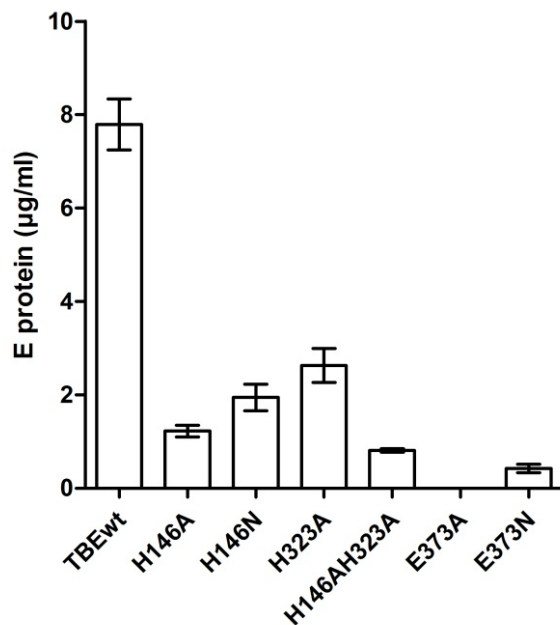


Figure 25: E protein concentrations of cell culture supernatant 48 hours post transfection

Quantification of the E protein concentration in cell culture supernatants 48 hours post transfection. Mean values of 3 independent ELISA measurements of one representative electroporation are shown, error bars represent SD.

Since it was not clear in which form (soluble, RSP or incorporated into whole virus particles) the E protein was present in the cell culture supernatants, analysis by rate zonal gradient centrifugation was performed as described in Materials and Methods (Figure 26). Purified virions, which were run in parallel as a control, sedimented in fractions 12-15.

The E protein was detected in the top fractions of all cell culture supernatants (histidine mutants and wt) which indicated soluble, nonintegrated E. Only in the case of the H323A mutant and wt, the E protein was also detected in the fractions corresponding to virus particles (20% and 25% of total E protein for H323A and wt, respectively).

Unfortunately, the sensitivity of the detection method was not sufficient to detect the viral peak for the other mutants.

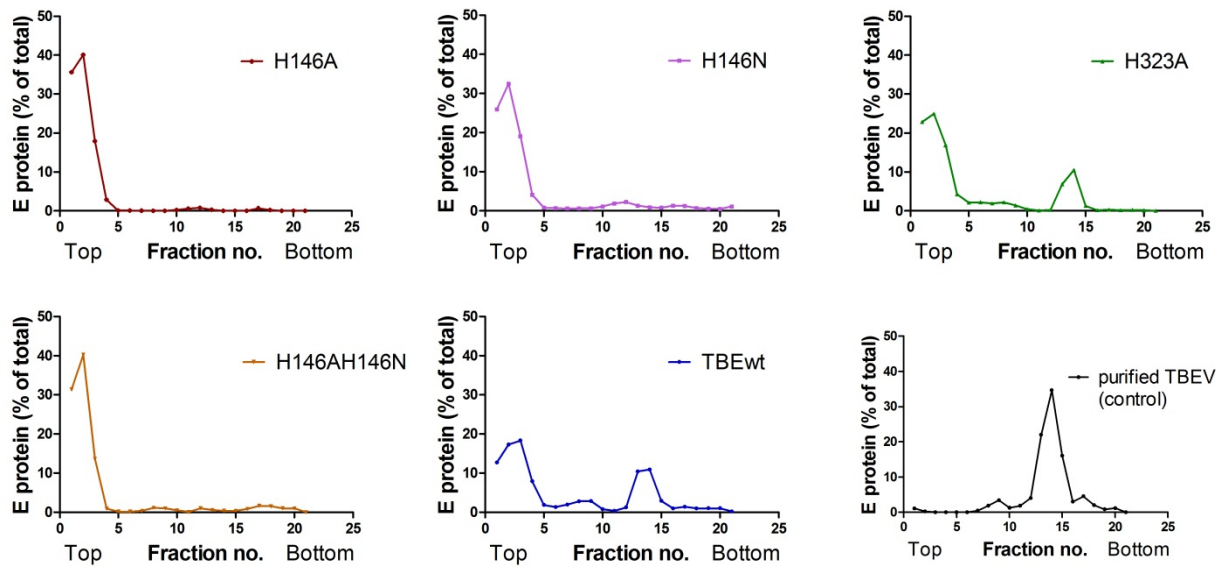


Figure 26: Analysis of particle formation by rate zonal gradient centrifugation

Sedimentation analysis of supernatants from cells transfected with wt and mutant RNAs. The particle sedimentation direction is from left to right. Results are expressed as percentage of E protein found in the fractions in relation to the total amount of E in the gradient.

5.2.2.4 Analysis of resuscitating mutations

To investigate whether passaging of mutants resulted in resuscitating mutations and to examine mutant virus stability, serial passages of cell culture supernatants from transfected cells were performed. A total of four passages were carried out. Cell culture supernatant from the last passage was used for RNA isolation, cDNA synthesis and sequencing of the structural proteins as described in Materials and Methods. This supernatant was also used for infections of fresh cells (fifth passage) and immunofluorescence staining.

No resuscitating mutations or additional mutations were found after four serial passages and immunofluorescence staining of infected cells in the fifth passage corresponded to infected cells of the first passage (compared in Figure 27).

Taken together, the viruses containing the engineered modifications were stable, during five serial passages.

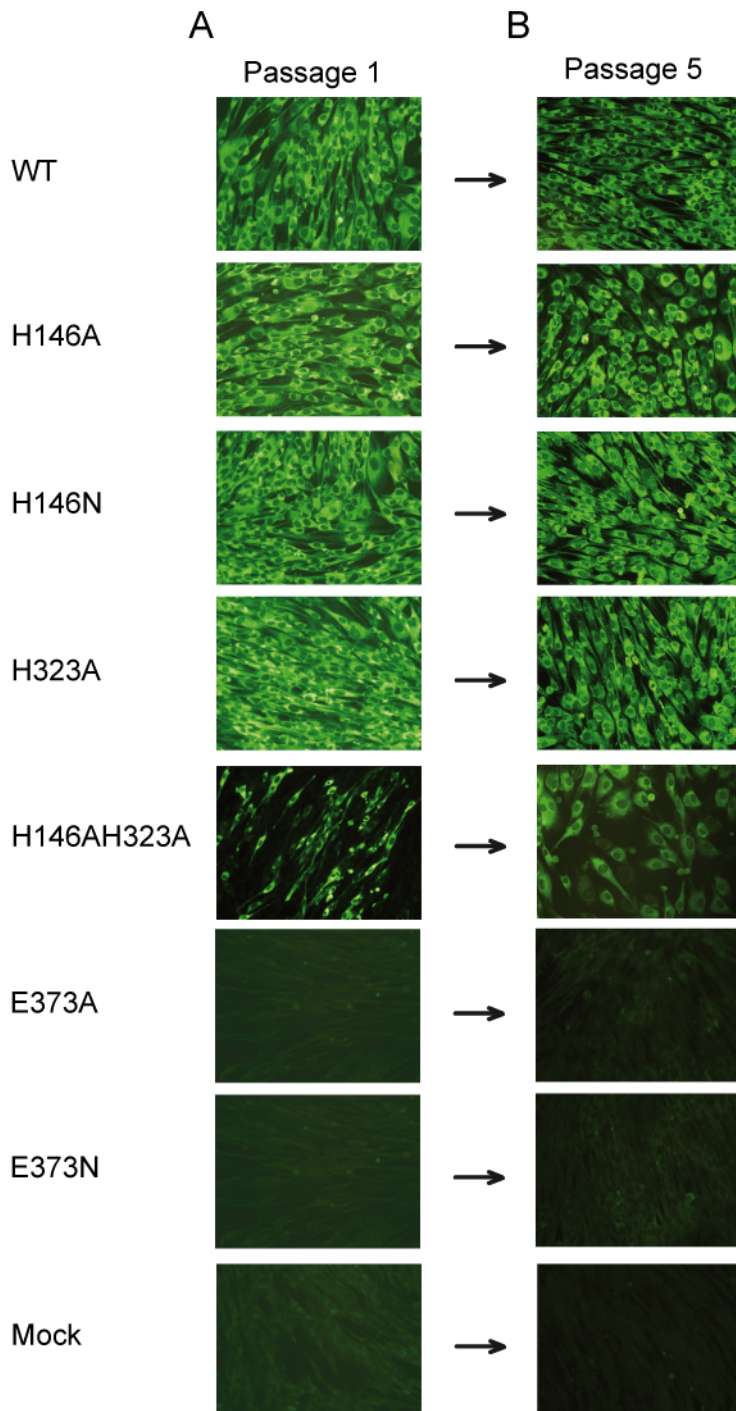


Figure 27: Immunofluorescence staining of BHK-21 cells after (A) first and (B) fifth passage

(A) Immunofluorescence pictures from BHK-21 cells infected with cell culture supernatants harvested 48 hours after transfection. (B) Immunostaining of cells infected with the supernatants after the fourth passage. Staining was performed using a polyclonal serum recognizing the structural proteins of TBEV. Immunofluorescence pictures from one representative electroporation are shown.

6 Discussion

6.1 Analysis of the functional relevance of the transmembrane hairpin of flavivirus in membrane fusion

The double membrane anchor of the envelope protein E (consisting of two antiparallel helices, TM1 and TM2) is a unique distinguishing structural feature of the flavivirus fusion protein. The TM2 helix is a remnant of flavivirus polyprotein processing and acts as an internal signal sequence for the synthesis of the NS1 protein (Lindenbach 2007). All other viral fusion proteins analyzed so far possess single TM anchors that are C-terminally extended by intracytoplasmic tails of various lengths (White, Delos et al. 2008). Membrane anchor modifications of class I and class III fusion proteins affected late stages of fusion, such as the hemifusion state and/or the opening of the fusion pore (Langosch, Hofmann et al. 2007; White, Delos et al. 2008).

Studies with mutant RSPs of TBEV revealed that the TM2 helix is multifunctional and not only essential for viral polyprotein processing but also indispensable for efficient membrane fusion (Fritz, Blazevic et al. 2011). The engineered modifications of the transmembrane anchor of the E protein include the deletion of TM2, the replacement of both TM domains by those of the related JEV, and the chimerization of membrane anchors (TBEV-JEV). None of the designed TM-mutations affected early steps of the fusion process, but TM-interactions apparently contributed to the stability of the post-fusion E trimer and the completion of the membrane merger.

Unfortunately, it was not possible to extend the findings obtained in the RSP system to infectious virus and to study of whole virions in the same assays. As shown in this thesis, the engineering of recombinant TBE viruses with completely heterologous TMs or chimeric TMs resulted in a severe impairment of virus production and recoveries that were 4, 5, and 6 logs lower compared to wt with JE TM1-JE TM2, TBE TM1-JE TM2, and JE TM1-TBE TM2 TM-mutants, respectively. There are several possible explanations for these findings: In the case of the chimeric TM anchor mutant viruses, reduced fusion activities as observed with the RSPs could contribute to the low infectivities. However, also the specific infectivity of the JE TM1-JE TM2 mutant viruses was dramatically reduced and revealed a ~10,000 times lower yield compared to wt, although the same mutation had no effect on the fusion activity of RSP JE1-JE2. It has therefore to be assumed that modifications of the TM hairpin of the E protein in the virus also affected other steps of the virus life cycle, independent of membrane fusion.

Particle assembly would be a possible candidate for such effects, involving mechanisms that contribute to virion but not to subviral particle formation. RSPs can be formed through lateral

interactions between prM-E heterodimers only and they are smaller than whole virions (Schalich, Allison et al. 1996). In mature RSPs, the protein E homodimers are organized in a regular T=1 icosahedral lattice (Ferlenghi, Clarke et al. 2001) whereas on the viral surface the E proteins are more tightly packed in a herringbone-like arrangement (Figure 5) (Kuhn, Zhang et al. 2002; Mukhopadhyay, Kim et al. 2003). It is possible that the more complex organization of the viral envelope requires interactions of the TMDs of prM-E heterodimers during virus particle assembly and/or budding that are dispensable for RSP formation. Such an interpretation would be consistent with previous studies that had demonstrated that alterations in the transmembrane anchor of the E protein could severely impair the production of infectious viruses (Op De Beeck, Rouille et al. 2004; Orlinger, Hoenninger et al. 2006; Hsieh, Tsai et al. 2010).

Irrespective of the possible involvement of the double transmembrane anchor of the E protein in virus assembly, these TM helices play an essential role in the late steps of flavivirus membrane fusion and provide both intra- and intermolecular protein E trimer interactions that are necessary to drive the fusion process to completion. This is an extension of the already existing models of flavivirus fusion that have focused on the relocation of protein E DIII and the zippering of the stem region only to serve as primary energy sources for this process (Harrison 2008).

6.2 Investigation of key residues of the E protein involved in triggering membrane fusion

The mutational analysis of histidines conserved among all flavivirus E proteins – using RSPs of TBEV – provided evidence that H323 is part of the pH sensor necessary for triggering low-pH-induced flavivirus membrane fusion (Fritz, Stiasny et al. 2008). This amino acid is located at the DI/DIII interface which contains a network of interactions between the two domains in the E protein monomer of the pre-fusion dimer (hydrogen bonds, van der Waals contacts) and a salt bridge between R9 (DI) and E373 (DIII). Domains I and III of the E protein provide a pocket for the FP at the tip of the partner subunit. The destabilization of this interface by protonation is essential for the release of the FP as well as for the relocation of DIII and thus for the entire fusion process. Understanding the details of the flavivirus membrane fusion process at a molecular level can help in the search for antiviral compounds that target structural transitions during fusion (Stiasny, Fritz et al. 2009).

In the context of single round particles (SIPs) of West Nile virus (WNV), SIPs containing mutated histidines were still able to infect cells. Some of the identified mutants were less

infectious than wt SIPs (Nelson, Poddar et al. 2009), but specific infectivities of the mutated SIPs have not been determined. A possible explanation for the observed infectivity – despite the replacement of histidines – could be that other residues take over the pH sensor function in the course of the infection of the host cell. The local protein environment can change the pKa of titrable side chains (Srivastava, Barber et al. 2007) in such a way that aspartates and glutamates could function as alternative pH sensors, e.g. the highly conserved E373 (DIII) which forms a salt bridge with R9 (DI) in the pre-fusion dimer.

To study the possible discrepancy between the fusion data obtained with RSPs of TBEV and infectivity of SIPs of WNV, standardized infectivity assays and in vitro fusion experiments with viruses and RSPs containing mutations of conserved residues at the DI/DIII interface of the E protein are necessary. Such TBEV mutants have been generated during this diploma thesis and the infectivities of these viruses were determined.

In the RSP system, the H323A mutant was strongly impaired in membrane fusion and mutating residue H146 abolished secretion of RSPs (Fritz, Stiasny et al. 2008). In the infectious system, the single mutants (TBEV H323A, H146A, and H146N) were still infectious, although a 10-fold reduced infectivity compared to wt was detected. The combination of both mutations (TBEV H146A-H323A) revealed even a 100-fold reduced infectivity compared to wt.

Characterization of the cell culture supernatant using rate zonal gradient centrifugation revealed particles comparable to wt only for the TBEV H323A mutant. In the case of the other mutants it remained unclear whether the amounts of produced viral particles were below the detection limit of the analysis, especially for the H146A-H323A double mutant with the lowest infectivity titers, or whether the produced mutant virus particles were less stable and disintegrated during rate zonal gradient centrifugation.

We also attempted to mutate the conserved residue E373 which is part of the salt bridge between DI and DIII and could act as an alternative pH sensor in the acidic endosomal compartments. Unfortunately, the replacement of E373 by either A or N completely abolished the secretion of E and infectivity, indicating that E373 is already necessary for proper formation and/or secretion of virus particles.

At present it is unclear whether the observed reduced infectivities were due to an impairment in fusion or other steps of the viral life cycle. To address this issue, upscaling of virus productions is necessary followed by quality controls of the mutants including particle formation, maturation state and folding of E in comparison to wt. Such well characterized virus particles can then be used for the determination of fusion activities and specific infectivities.

7 References

- Allison, S. L., J. Schalich, et al. (2001). "Mutational evidence for an internal fusion peptide in flavivirus envelope protein E." *J Virol* **75**(9): 4268-4275.
- Allison, S. L., K. Stadler, et al. (1995). "Synthesis and secretion of recombinant tick-borne encephalitis virus protein E in soluble and particulate form." *J Virol* **69**(9): 5816-5820.
- Allison, S. L., K. Stiasny, et al. (1999). "Mapping of functional elements in the stem-anchor region of tick-borne encephalitis virus envelope protein E." *J Virol* **73**(7): 5605-5612.
- Backovic, M. and T. S. Jardetzky (2009). "Class III viral membrane fusion proteins." *Curr Opin Struct Biol* **19**(2): 189-196.
- Barrett, P. N., Plotkin, S.A., Ehrlich, H.J. (2008). Tick-borne encephalitis virus vaccines. *Vaccines*. S. A. Plotkin, Orenstein, W.A., Offit, P.A., Saunders Elsevier.
- Berger, A. (2009). Establishing a trans-packaging system for TBEV replicons to study events of complementation and recombination in the genus Flavivirus.
- Bressanelli, S., K. Stiasny, et al. (2004). "Structure of a flavivirus envelope glycoprotein in its low-pH-induced membrane fusion conformation." *Embo J* **23**(4): 728-738.
- Chambers, T. J., C. S. Hahn, et al. (1990). "Flavivirus genome organization, expression, and replication." *Annu Rev Microbiol* **44**: 649-688.
- Cherrier, M. V., B. Kaufmann, et al. (2009). "Structural basis for the preferential recognition of immature flaviviruses by a fusion-loop antibody." *EMBO J* **28**(20): 3269-3276.
- Corver, J., A. Ortiz, et al. (2000). "Membrane fusion activity of tick-borne encephalitis virus and recombinant subviral particles in a liposomal model system." *Virology* **269**(1): 37-46.
- Donoso Mantke, O., R. Schadler, et al. (2008). "A survey on cases of tick-borne encephalitis in European countries." *Euro Surveill* **13**(17).
- Ecker, M., S. L. Allison, et al. (1999). "Sequence analysis and genetic classification of tick-borne encephalitis viruses from Europe and Asia." *J Gen Virol* **80** (Pt 1): 179-185.
- Elshuber, S., S. L. Allison, et al. (2003). "Cleavage of protein prM is necessary for infection of BHK-21 cells by tick-borne encephalitis virus." *J Gen Virol* **84**(Pt 1): 183-191.
- Fauquet, C. M., Mayo, M.A. (2005). The positive sense single stranded RNA viruses. *Virus Taxonomy, Classification and Nomenclature of Viruses, 8th Report of the International Committee on Taxonomy of Viruses*. C. M. Fauquet, Mayo, M.A., Maniloff, J., Desselberger, U., Ball, L.A., ELSEVIER academic press.
- Ferlenghi, I., M. Clarke, et al. (2001). "Molecular organization of a recombinant subviral particle from tick-borne encephalitis virus." *Mol Cell* **7**(3): 593-602.
- Fischer, M., C. Casey, et al. (2007). "Promise of new Japanese encephalitis vaccines." *Lancet* **370**(9602): 1806-1808.
- Fritz, R. (2009). Molecular dissection of flavivirus membrane fusion by structure-based mutational analysis.
- Fritz, R., J. Blazevic, et al. (2011). "The unique transmembrane hairpin of the flavivirus fusion protein E is essential for membrane fusion." *J Virol*, paper in press.
- Fritz, R., K. Stiasny, et al. (2008). "Identification of specific histidines as pH sensors in flavivirus membrane fusion." *J Cell Biol* **183**(2): 353-361.
- Gollins, S. W. and J. S. Porterfield (1986). "pH-dependent fusion between the flavivirus West Nile and liposomal model membranes." *J Gen Virol* **67** (Pt 1): 157-166.
- Gubler, D. J., Kuno G., Markoff, L. (2007). Flaviviruses. *Fields Virology, 5th ed. Lippincott Williams & Wilkins Co., Philadelphia, PA*. D. M. Knipe, Howley, P.M. Philadelphia: 1153-1252.
- Haglund, M. and G. Gunther (2003). "Tick-borne encephalitis--pathogenesis, clinical course and long-term follow-up." *Vaccine* **21 Suppl 1**: S11-18.
- Harrison, S. C. (2008). "The pH sensor for flavivirus membrane fusion." *J Cell Biol* **183**(2): 177-179.
- Harrison, S. C. (2008). "Viral membrane fusion." *Nat Struct Mol Biol* **15**(7): 690-698.
- Heinz, F. X., H. Holzmann, et al. (2007). "Field effectiveness of vaccination against tick-borne encephalitis." *Vaccine* **25**(43): 7559-7567.

- Heinz, F. X., K. Stiasny, et al. (1994). "Structural changes and functional control of the tick-borne encephalitis virus glycoprotein E by the heterodimeric association with protein prM." *Virology* **198**(1): 109-117.
- Holzmann, H. (2003). "Diagnosis of tick-borne encephalitis." *Vaccine* **21 Suppl 1**: S36-40.
- Hsieh, S. C., W. Y. Tsai, et al. (2010). "The Length of and Nonhydrophobic Residues in the Transmembrane Domain of Dengue Virus Envelope Protein Are Critical for Its Retention and Assembly in the Endoplasmic Reticulum." *Journal of Virology* **84**(9): 4782-4797.
- Junjhon, J., T. J. Edwards, et al. (2010). "Influence of pr-M cleavage on the heterogeneity of extracellular dengue virus particles." *J Virol* **84**(16): 8353-8358.
- Kampmann, T., D. S. Mueller, et al. (2006). "The Role of histidine residues in low-pH-mediated viral membrane fusion." *Structure* **14**(10): 1481-1487.
- Kanai, R., K. Kar, et al. (2006). "Crystal structure of west nile virus envelope glycoprotein reveals viral surface epitopes." *J Virol* **80**(22): 11000-11008.
- Kandolf, R. and P. H. Hofschneider (1985). "Molecular cloning of the genome of a cardiotropic Coxsackie B3 virus: full-length reverse-transcribed recombinant cDNA generates infectious virus in mammalian cells." *Proc Natl Acad Sci U S A* **82**(14): 4818-4822.
- Kaufmann, B. and M. G. Rossmann (2010). "Molecular mechanisms involved in the early steps of flavivirus cell entry." *Microbes Infect.*
- Kielian, M. (2006). "Class II virus membrane fusion proteins." *Virology* **344**(1): 38-47.
- Kiermayr, S., K. Stiasny, et al. (2009). "Impact of quaternary organization on the antigenic structure of the tick-borne encephalitis virus envelope glycoprotein E." *J Virol* **83**(17): 8482-8491.
- Kofler, R. M., F. X. Heinz, et al. (2002). "Capsid protein C of tick-borne encephalitis virus tolerates large internal deletions and is a favorable target for attenuation of virulence." *J Virol* **76**(7): 3534-3543.
- Kofler, R. M., V. M. Hoenninger, et al. (2006). "Functional analysis of the tick-borne encephalitis virus cyclization elements indicates major differences between mosquito-borne and tick-borne flaviviruses." *J Virol* **80**(8): 4099-4113.
- Kroschewski, H., S. L. Allison, et al. (2003). "Role of heparan sulfate for attachment and entry of tick-borne encephalitis virus." *Virology* **308**(1): 92-100.
- Kuhn, R. J., W. Zhang, et al. (2002). "Structure of dengue virus: implications for flavivirus organization, maturation, and fusion." *Cell* **108**(5): 717-725.
- Kuno, G., G. J. Chang, et al. (1998). "Phylogeny of the genus *Flavivirus*." *J Virol* **72**(1): 73-83.
- Langosch, D., M. Hofmann, et al. (2007). "The role of transmembrane domains in membrane fusion." *Cell Mol Life Sci* **64**(7-8): 850-864.
- Lindenbach, B. D., Thiel, H.-J., Rice, C.M. (2007). *Flaviviridae: the viruses and their replication*. *Fields Virology, 5th ed.* Lippincott Williams & Wilkins Co., Philadelphia, PA. D. M. Knipe, Howley, P.M. Philadelphia: 1101-1152.
- Lindquist, L. and O. Vapalahti (2008). "Tick-borne encephalitis." *Lancet* **371**(9627): 1861-1871.
- Lorenz, I. C., S. L. Allison, et al. (2002). "Folding and dimerization of tick-borne encephalitis virus envelope proteins prM and E in the endoplasmic reticulum." *J Virol* **76**(11): 5480-5491.
- Mackenzie, J. S., D. J. Gubler, et al. (2004). "Emerging flaviviruses: the spread and resurgence of Japanese encephalitis, West Nile and dengue viruses." *Nat Med* **10**(12 Suppl): S98-109.
- Mandl, C. W., M. Ecker, et al. (1997). "Infectious cDNA clones of tick-borne encephalitis virus European subtype prototypic strain Neudoerfl and high virulence strain Hypr." *J Gen Virol* **78 (Pt 5)**: 1049-1057.
- Mandl, C. W., F. X. Heinz, et al. (1988). "Sequence of the structural proteins of tick-borne encephalitis virus (western subtype) and comparative analysis with other flaviviruses." *Virology* **166**(1): 197-205.

- Mandl, C. W., F. X. Heinz, et al. (1989). "Genome sequence of tick-borne encephalitis virus (Western subtype) and comparative analysis of nonstructural proteins with other flaviviruses." *Virology* **173**(1): 291-301.
- Martens, S. and H. T. McMahon (2008). "Mechanisms of membrane fusion: disparate players and common principles." *Nat Rev Mol Cell Biol* **9**(7): 543-556.
- Modis, Y., S. Ogata, et al. (2003). "A ligand-binding pocket in the dengue virus envelope glycoprotein." *Proc Natl Acad Sci U S A* **100**(12): 6986-6991.
- Modis, Y., S. Ogata, et al. (2004). "Structure of the dengue virus envelope protein after membrane fusion." *Nature* **427**(6972): 313-319.
- Modis, Y., S. Ogata, et al. (2005). "Variable surface epitopes in the crystal structure of dengue virus type 3 envelope glycoprotein." *J Virol* **79**(2): 1223-1231.
- Moesker, B., I. A. Rodenhuis-Zybert, et al. (2010). "Characterization of the functional requirements of West Nile virus membrane fusion." *J Gen Virol* **91**(Pt 2): 389-393.
- Mueller, D. S., T. Kampmann, et al. (2008). "Histidine protonation and the activation of viral fusion proteins." *Biochem Soc Trans* **36**(Pt 1): 43-45.
- Mukhopadhyay, S., B. S. Kim, et al. (2003). "Structure of West Nile virus." *Science* **302**(5643): 248.
- Mukhopadhyay, S., R. J. Kuhn, et al. (2005). "A structural perspective of the flavivirus life cycle." *Nat Rev Microbiol* **3**(1): 13-22.
- Nayak, V., M. Dessau, et al. (2009). "Crystal structure of dengue virus type 1 envelope protein in the postfusion conformation and its implications for membrane fusion." *J Virol* **83**(9): 4338-4344.
- Nelson, S., S. Poddar, et al. (2009). "Protonation of individual histidine residues is not required for the pH-dependent entry of west nile virus: evaluation of the "histidine switch" hypothesis." *J Virol* **83**(23): 12631-12635.
- Nowak, T., P. M. Farber, et al. (1989). "Analyses of the terminal sequences of West Nile virus structural proteins and of the in vitro translation of these proteins allow the proposal of a complete scheme of the proteolytic cleavages involved in their synthesis." *Virology* **169**(2): 365-376.
- Nybakken, G. E., C. A. Nelson, et al. (2006). "Crystal structure of the West Nile virus envelope glycoprotein." *J Virol* **80**(23): 11467-11474.
- Op De Beeck, A., Y. Rouille, et al. (2004). "The transmembrane domains of the prM and E proteins of yellow fever virus are endoplasmic reticulum localization signals." *J Virol* **78**(22): 12591-12602.
- Orlinger, K. (2007). Construction and Application of Bicostronic Flaviviruses.
- Orlinger, K. K., V. M. Hoenninger, et al. (2006). "Construction and mutagenesis of an artificial bicistronic tick-borne encephalitis virus genome reveals an essential function of the second transmembrane region of protein e in flavivirus assembly." *J Virol* **80**(24): 12197-12208.
- Qin, Z. L., Y. Zheng, et al. (2009). "Role of conserved histidine residues in the low-pH dependence of the Semliki Forest virus fusion protein." *J Virol* **83**(9): 4670-4677.
- Rey, F. A., F. X. Heinz, et al. (1995). "The envelope glycoprotein from tick-borne encephalitis virus at 2 Å resolution." *Nature* **375**(6529): 291-298.
- Roche, S., A. A. Albertini, et al. (2008). "Structures of vesicular stomatitis virus glycoprotein: membrane fusion revisited." *Cell Mol Life Sci* **65**(11): 1716-1728.
- Roussel, A., J. Lescar, et al. (2006). "Structure and interactions at the viral surface of the envelope protein E1 of Semliki Forest virus." *Structure* **14**(1): 75-86.
- Sanger, F., S. Nicklen, et al. (1977). "DNA sequencing with chain-terminating inhibitors." *Proc Natl Acad Sci U S A* **74**(12): 5463-5467.
- Sapir, A., O. Avinoam, et al. (2008). "Viral and developmental cell fusion mechanisms: conservation and divergence." *Dev Cell* **14**(1): 11-21.
- Schalich, J., S. L. Allison, et al. (1996). "Recombinant subviral particles from tick-borne encephalitis virus are fusogenic and provide a model system for studying flavivirus envelope glycoprotein functions." *J Virol* **70**(7): 4549-4557.
- Schibli, D. J. and W. Weissenhorn (2004). "Class I and class II viral fusion protein structures reveal similar principles in membrane fusion." *Mol Membr Biol* **21**(6): 361-371.

- Schrauf, S. (2006). Mutational Analysis of the C-Terminal Region of the Capsid Protein of the Flavivirus TBEV.
- Schrauf, S., P. Schlick, et al. (2008). "Functional analysis of potential carboxy-terminal cleavage sites of tick-borne encephalitis virus capsid protein." *J Virol* **82**(5): 2218-2229.
- Smith, T. J., W. E. Brandt, et al. (1970). "Physical and biological properties of dengue-2 virus and associated antigens." *J Virol* **5**(4): 524-532.
- Solomon, T. and D. W. Vaughn (2002). "Pathogenesis and clinical features of Japanese encephalitis and West Nile virus infections." *Curr Top Microbiol Immunol* **267**: 171-194.
- Srivastava, J., D. L. Barber, et al. (2007). "Intracellular pH sensors: design principles and functional significance." *Physiology (Bethesda)* **22**: 30-39.
- Stadler, K., S. L. Allison, et al. (1997). "Proteolytic activation of tick-borne encephalitis virus by furin." *J Virol* **71**(11): 8475-8481.
- Stevens, J., A. L. Corper, et al. (2004). "Structure of the uncleaved human H1 hemagglutinin from the extinct 1918 influenza virus." *Science* **303**(5665): 1866-1870.
- Stiasny, K., S. L. Allison, et al. (2002). "Membrane interactions of the tick-borne encephalitis virus fusion protein E at low pH." *J Virol* **76**(8): 3784-3790.
- Stiasny, K., R. Fritz, et al. (2009). "Molecular mechanisms of flavivirus membrane fusion." *Amino Acids*.
- Stiasny, K. and F. X. Heinz (2006). "Flavivirus membrane fusion." *J Gen Virol* **87**(Pt 10): 2755-2766.
- Stiasny, K., S. Kiermayr, et al. (2006). "Cryptic properties of a cluster of dominant flavivirus cross-reactive antigenic sites." *J Virol* **80**(19): 9557-9568.
- Stiasny, K., C. Kossel, et al. (2005). "Differences in the postfusion conformations of full-length and truncated class II fusion protein E of tick-borne encephalitis virus." *J Virol* **79**(10): 6511-6515.
- Stiasny, K., C. Kossel, et al. (2007). "Characterization of a structural intermediate of flavivirus membrane fusion." *PLoS Pathog* **3**(2): e20.
- Stollar, V. (1969). "Studies on the nature of dengue viruses. IV. The structural proteins of type 2 dengue virus." *Virology* **39**(3): 426-438.
- Taucher, C. (2009). Recombination and packaging of flaviviruses.
- Taucher, C., A. Berger, et al. (2010). "A trans-complementing recombination trap demonstrates a low propensity of flaviviruses for intermolecular recombination." *J Virol* **84**(1): 599-611.
- Umareddy, I., O. Pluquet, et al. (2007). "Dengue virus serotype infection specifies the activation of the unfolded protein response." *Virol J* **4**: 91.
- Weissenhorn, W., A. Hinz, et al. (2007). "Virus membrane fusion." *FEBS Lett* **581**(11): 2150-2155.
- White, J. M., S. E. Delos, et al. (2008). "Structures and mechanisms of viral membrane fusion proteins: multiple variations on a common theme." *Crit Rev Biochem Mol Biol* **43**(3): 189-219.
- Yu, I. M., W. Zhang, et al. (2008). "Structure of the immature dengue virus at low pH primes proteolytic maturation." *Science* **319**(5871): 1834-1837.
- Zhang, W., P. R. Chipman, et al. (2003). "Visualization of membrane protein domains by cryo-electron microscopy of dengue virus." *Nat Struct Biol* **10**(11): 907-912.
- Zhang, Y., W. Zhang, et al. (2004). "Conformational changes of the flavivirus E glycoprotein." *Structure* **12**(9): 1607-1618.

Appendix

zjv00911/zjv4462d11z | xppws | S=1 | 3/11/11 | 4/C Fig: 1,6 | Art: 2458-10

zjs / DOCHHEAD=ARTICLE | zjss / DOCTOPIC=VIRUS-CELL INTERACTIONS
FROM COVER SHEET: Editor: Doms | Article No.: T | Section: InteractionsJOURNAL OF VIROLOGY, May 2011, p. 000
0022-538X/11/\$12.00 doi:10.1128/JVI.02458-10
Copyright © 2011, American Society for Microbiology. All Rights Reserved.

Vol. 85, No. 9

The Unique Transmembrane Hairpin of Flavivirus Fusion Protein E Is Essential for Membrane Fusion[∇]Richard Fritz,[†] Janja Blazevic, Christian Taucher,[‡] Karen Pangerl,
Franz X. Heinz, and Karin Stiasny*

Department of Virology, Medical University of Vienna, Vienna, Austria

Received 24 November 2010/Accepted 7 February 2011

The fusion of enveloped viruses with cellular membranes is mediated by proteins that are anchored in the lipid bilayer of the virus and capable of triggered conformational changes necessary for driving fusion. The flavivirus envelope protein E is the only known viral fusion protein with a double membrane anchor, consisting of two antiparallel transmembrane helices (TM1 and TM2). TM1 functions as a stop-transfer sequence and TM2 as an internal signal sequence for the first nonstructural protein during polyprotein processing. The possible role of this peculiar C-terminal helical hairpin in membrane fusion has not been investigated so far. We addressed this question by studying TM mutants of tick-borne encephalitis virus (TBEV) recombinant subviral particles (RSPs), an established model system for flavivirus membrane fusion. The engineered mutations included the deletion of TM2, the replacement of both TM domains (TMDs) by those of the related Japanese encephalitis virus (JEV), and the use of chimeric TBEV-JEV membrane anchors. Using these mutant RSPs, we provide evidence that TM2 is not just a remnant of polyprotein processing but, together with TM1, plays an active role in fusion. None of the TM mutations, including the deletion of TM2, affected early steps of the fusion process, but TM interactions apparently contribute to the stability of the postfusion E trimer and the completion of the merger of the membranes. Our data provide evidence for both intratrimer and intertrimer interactions mediated by the TMDs of E and thus extend the existing models of flavivirus membrane fusion.

Fn2 Membrane fusion is a crucial step during the cell entry of enveloped viruses and is mediated by specific membrane-anchored viral surface proteins (fusion proteins) (11, 24). According to their molecular architecture, these have been assigned to three different structural classes (classes I, II, and III) (11, 41). They all drive fusion by conformational changes that are triggered by interactions with the host cell (such as receptor binding or exposure to acidic pH) and presumably involve protein-protein interactions at the fusion site (41). Classes I and III, and the class II fusion proteins of alphaviruses, possess a single transmembrane (TM) domain that functions as a membrane anchor and is followed by a cytoplasmic tail of varying length (41). In contrast, the flavivirus class II viral fusion protein E is unique in possessing a hairpin-like double-membrane-spanning carboxy terminus, derived from a special combination of stop-transfer and internal signal sequences, required for the intracellular sorting and processing of the flaviviral polyprotein (21) (Fig. 1A).

F1 Flaviviruses are members of the genus *Flavivirus* (family *Flaviviridae*) and comprise a number of important human pathogens, including the dengue viruses, Japanese encephalitis virus (JEV), yellow fever virus, West Nile virus, and tick-borne

encephalitis virus (TBEV) (10, 40). They are small, enveloped, positive-strand RNA viruses that are assembled in the endoplasmic reticulum (ER) in an immature noninfectious form containing three structural proteins designated C (capsid), prM (precursor of M [membrane]), and E (envelope). During exocytosis, the prM protein is proteolytically cleaved by furin in the *trans*-Golgi network, and the C-terminal membrane-bound cleavage product of prM (M) remains associated with mature secreted virions (43, 44). As revealed by cryo-electron microscopy (cryo-EM), immature and mature viruses display different envelope protein organizations, but both have icosahedral symmetry, with a specific arrangement of 60 trimers of prM-E heterodimers and 90 E dimers, respectively (14). E functions as both a receptor binding and a fusion protein, and the atomic structures of C-terminally truncated soluble forms of E (sE) have been determined in their pre- and postfusion conformations for several flaviviruses (35). sE is composed of three distinct domains (DI, DII, and DIII), and an S-S bridge stabilized loop at the tip of DII functions as the fusion peptide (FP) (Fig. 1A). The organization of the C-terminal part of the molecule—not present in the X-ray structures—was elucidated by cryo-EM of mature dengue virions (45). It is composed of two mostly amphipathic alpha helices that are half buried in the outer leaflet of the viral membrane (designated the “stem”) and connect the E ectodomain to the C-terminal transmembrane elements (TM1 and TM2 helices) (Fig. 1A). These are arranged in an antiparallel coiled-coil hairpin structure linked by four to six mostly polar amino acids (45) and display only a low degree of sequence conservation among flaviviruses (Fig. 1D). Both have important functions during biosynthesis and processing of the viral polyprotein, with the TM1 element

* Corresponding author. Mailing address: Department of Virology, Medical University of Vienna, Kinderspitalgasse 15, 1095, Vienna, Austria. Phone: 43-1-40160, ext. 65505. Fax: 43-1-40160, ext. 965 599. E-mail: karin.stiasny@meduniwien.ac.at.

[†] Present address: Baxter BioScience, Biomedical Research Center, Uferstrasse 15, 2304 Orth/Donau, Austria.

[‡] Present address: Intercell AG, Campus Vienna Biocenter 3, 1030 Vienna, Austria.

[∇] Published ahead of print on ●●●●●●●●.

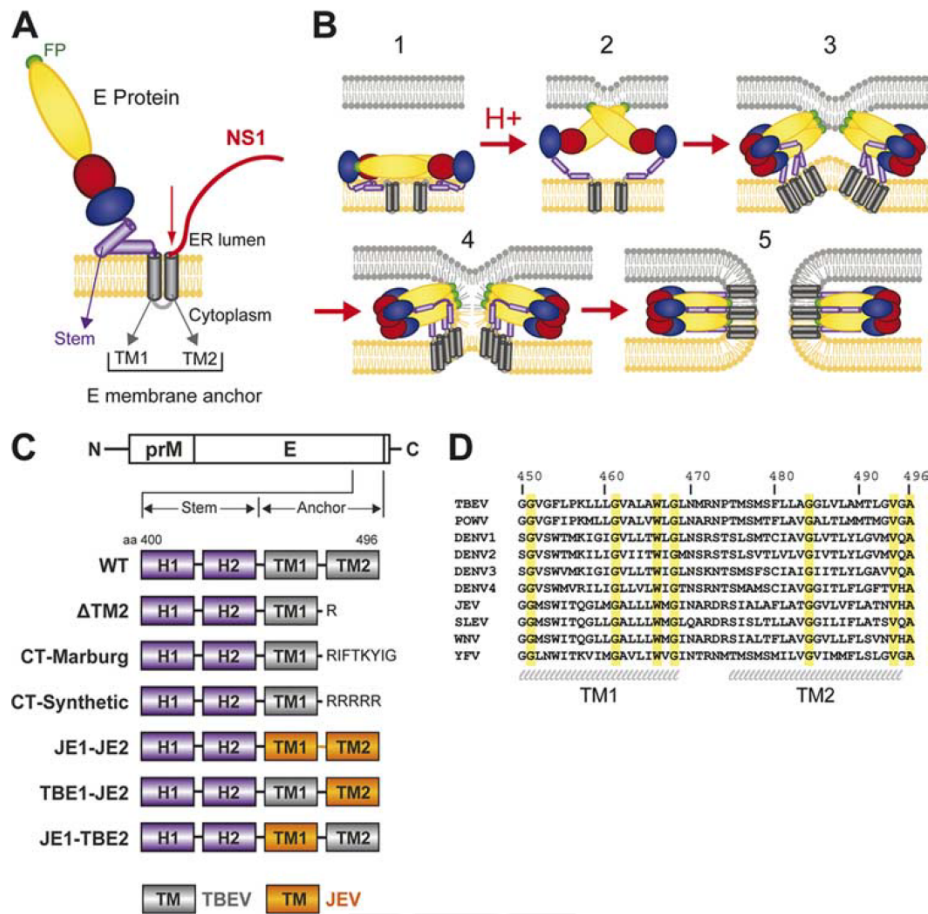


FIG. 1. Representations of the flavivirus E protein (A), membrane fusion (B), modifications engineered into the transmembrane (TM) region of E (C), and sequence alignment of TM regions of E (D). (A) Membrane topologies of E and NS1 during polyprotein processing at the ER membrane. TM2 functions as an internal signal sequence for NS1. The red arrow indicates host signalase cleavage at the E-NS1 junction. Color code for E: domain I, red; domain II, yellow; domain III, blue; stem, purple; anchor, gray; FP, green. (B) Flavivirus membrane fusion. 1, side view of an E dimer at the surface of a flavivirus particle at neutral pH; 2, low-pH-induced E dimer dissociation, extension of the stem, and interaction of the FPs with the target membrane; 3, E trimerization and initiation of hairpin formation (DIII relocates to the side of the molecule, and the stem zippers along the trimeric core); 4, formation of a stalk-like hemifusion intermediate with only the apposing leaflets merged; 5, formation of the hairpin-like postfusion structure and the opening of a fusion pore. The color code for E domains is as in panel A. Color code for membranes: viral membrane, orange; host cell membrane, gray. (C) Diagram showing C-terminal modifications of E in the constructs used for producing mutant RSPs. The numbers indicate amino acid (aa) positions. (D) Alignment of the amino acid sequences of the membrane anchor regions of several flavivirus E proteins (TBE numbering): TBEV (Genbank accession number U27495), Powassan virus (POWV) (Genbank accession number L06436), dengue virus (DENV) type 1 (Genbank accession number FJ687432), DENV type 2 (Genbank accession number NC_001474), DENV type 3 (Genbank accession number FJ850055), DENV type 4 (Genbank accession number AY618990), JEV (Genbank accession number EF571853), St. Louis encephalitis virus (SLV) (Genbank accession number M16614), West Nile virus (WNV) (Genbank accession number DQ211652), and yellow fever virus (YFV) (Genbank accession number AY640589). Identical amino acid residues are highlighted in yellow. The predicted TM1 and TM2 helices are indicated at the bottom.

serving as a stop-transfer sequence for E and the TM2 element as an internal signal sequence for the translocation of the first nonstructural protein (NS1) into the lumen of the ER (21) (Fig. 1A).

The existing models of flavivirus fusion are based on the pre- and postfusion structures of sE, as well as on biochemical studies (Fig. 1B). After virus uptake by receptor-mediated endocytosis, the low endosomal pH causes the exposure of the FPs and their insertion into the target membrane. Further changes involve trimerization of E and the formation of its hairpin-like postfusion structure with the FPs and the TM domains (TMDs) on the same side of the molecule. These

molecular rearrangements and interactions finally result in the opening of a fusion pore (reviewed in references 11, 14, and 36) (Fig. 1B). In the current flavivirus fusion models, the TMDs have not been ascribed a specific functional role, except for anchoring E in the viral membrane.

Since the presence of a double membrane anchor is a unique structural feature not found in other viral fusion proteins, it was the objective of our work to study the contributions of these sequence elements to the different stages of flavivirus membrane fusion. We were specifically interested in whether the TM2 helix is merely a functional remnant of polyprotein processing or whether it has an additional role in the fusion

process. As an experimental system, we chose noninfectious capsid-less recombinant subviral particles (RSPs) of TBE virus, because they have fusion characteristics similar to those of whole virions (6) and modifications of the double membrane anchor are uncoupled from the TM2 signal sequence function that would be required for virus replication. We modified the membrane anchor of E by deleting the TM2 helix, replacing both TMDs with those of a heterologous flavivirus (JEV), and shuffling the TMDs between TBEV and JEV. Functional analyses of these mutant RSPs demonstrate that the TM2 helix is completely dispensable for the early steps of membrane fusion (including FP exposure, interaction with target membranes, and E trimerization) but contributes to E trimer stability and is essential for later fusion steps, including the stage of hemifusion. Our data not only provide evidence for a role of the TMDs in intratrimer interactions, but also indicate the participation of TMDs in intertrimer interactions that are both required for efficient fusion.

MATERIALS AND METHODS

Virus sequences. The different constructs used in this study were based on Western subtype TBEV strain Neudoerfl (GenBank accession number U27495) and JEV strain Nakayama (GenBank accession number EF571853).

RSP plasmids and cloning procedures (Fig. 1C). SV-PE (wild type ([WT])) was the parent plasmid for mutant construction and WT controls (1). The plasmid contains nucleotides 388 to 2550 from TBEV and includes the last 31 codons of the C gene, the entire prM and E genes, and the first 30 codons of the NS1 gene under the control of the simian virus 40 early promoter. Construction of the Δ TM2 deletion mutant, in which a TAG stop codon replaces the codon for the amino acid at position 473 of the E gene of the SV-PE WT plasmid (3), was reported previously. Constructs containing cytoplasmic tails (CT) instead of the TM2 region and shuffled or heterologous anchors were generated by using unique restriction sites to introduce chemically synthesized DNA fragments (GeneArt) into the parent plasmid. The plasmids SV-PE CT-Marburg and SV-PE CT-Synthetic corresponded to SV-PE WT up to the codon of amino acid residue 472 of E, followed by the nucleotide sequences ATCTTTACTAAATA TATCGGATAG (Marburg) and AGAAGAAGATAG (Synthetic). These encode the cytoplasmic tail of the Marburg virus fusion protein (RIFTKYIG) and a synthetic oligo(R) sequence. In plasmid SV-PE JE1-JE2, the complete double-membrane-spanning anchor, including the short loop connecting the two helices of TBEV, was replaced by the corresponding JEV sequences, together with the first 30 codons of the NS1 gene. In SV-PE TBE1-JE2, the TBE TM2 domain plus the following NS1 sequence, and in SV-PE JE1-TBE2, the TBE TM1 domain, were replaced. In both constructs, the short loop between the two TM regions was derived from TBEV.

Production and quality controls of RSPs. For the production of RSPs, COS-1 cells were electroporated with the corresponding recombinant plasmids as described previously (33). Particles secreted into cell culture supernatants were harvested 48 h after electroporation by ultracentrifugation for 2 h at 44,000 rpm. The pelleted particles were resuspended in TAN buffer (50 mM triethanolamine [TEA], 100 mM NaCl, pH 8.0). For coflotation and lipid-mixing experiments, particles were subsequently purified by sucrose gradient centrifugation (2, 33). For lipid-mixing assays, the particles were metabolically labeled with 1-pyrenehexadecanoic acid (Molecular Probes; Invitrogen) as described previously (2, 6). RSPs secreted from transfected cells were quantified in a four-layer enzyme-linked immunosorbent assay (ELISA) after solubilization with 0.4% SDS at 65°C for 30 min (12). The hemagglutination (HA) activity of RSPs was measured at pH 6.4 by the method of Clarke and Casals, using goose erythrocytes (5). The structural integrity of the conformation of E on the particle surface was confirmed by epitope mapping with 22 E-specific monoclonal antibodies (MAbs) in ELISA (2, 16). To confirm that the mutations did not affect the intracellular maturation process, the presence of prM was analyzed in mutant RSPs and compared to the contents of WT particles by Western blotting as described previously (8).

Virus plasmids and cloning procedures. Plasmid pTNd/c contains a full-length genomic cDNA insert of TBEV strain Neudoerfl cloned into the vector pBR322 under the control of a T7 transcription promoter (23). The membrane anchor region of TBEV E in the pTNd/c vector was replaced by chemically synthesized

DNA fragments (GeneArt) containing the heterologous membrane anchor of JEV (TBEV JE1-JE2) or shuffled membrane anchors (TBEV JE1-TBE2 and TBEV TBE1-JE2) using unique restriction sites. In contrast to RSP mutants JE1-JE2 and TBE-JE2, the NS1 sequence was not replaced by that of JEV in the corresponding TBEV mutants. Full-length DNA templates for *in vitro* transcription of TBEV plasmids were generated as described previously (17).

RNA transfection and quantification. *In vitro* transcription and transfection of BHK-21 cells by electroporation were performed as described previously (39). Briefly, RNA was synthesized from full-length cDNA clones using the T7 Megascript kit (Ambion) according to the manufacturer's instructions. The template DNA was digested with DNase I, and the quality of the RNA was checked by electrophoresis in a 1% agarose gel containing 6% formalin. RNA was purified with an RNeasy minikit (Qiagen) and quantified spectrophotometrically, and equimolar amounts of the corresponding RNAs were used for the transfection of BHK cells. The number of particles containing genomic RNA (RNA equivalents) in the cell culture supernatant was determined 24 h posttransfection by quantitative PCR (qPCR) after reverse transcription of the viral RNA, as described previously (18).

Liposomes. Large unilamellar liposomes were prepared as described previously (37). Phosphatidylcholine, phosphatidylethanolamine (Avanti Polar Lipids), and cholesterol (Sigma-Aldrich) were mixed at a molar ratio of 1:1:2 in chloroform. The mixture was dried to a homogeneous film in high vacuum and hydrated in liposome buffer (10 mM TEA, 140 mM NaCl, pH 8.0) by 5 freeze-thaw cycles. Prior to use, liposomes were subjected to 21 extrusion cycles through polycarbonate membranes (200-nm pore size) using a LiposoFast-Basic extruder (Avestin).

Fusion assay. Fusion of pyrene-labeled RSPs with liposomes was measured by monitoring the decrease in pyrene excimer fluorescence caused by the dilution of pyrene-labeled phospholipids in the RSP membrane in the unlabeled liposome membrane (8). Briefly, pyrene-labeled RSPs were mixed with liposomes (total lipid, 0.3 mM) in a continuously stirred fluorimeter cuvette at 37°C. Lipid mixing was induced by adding 300 mM morpholinoethanesulfonic acid (MES) to yield a pH of 5.4. Fluorescence was continuously monitored by a Perkin-Elmer LS-50B fluorescence spectrophotometer. The initial excimer fluorescence after mixing was defined as 0% fusion. To determine the residual excimer fluorescence at infinite dilution of the probe (defined as 100% fusion for calculating the fusion extents), the detergent *n*-octa(ethylene glycol)*n*-dodecyl monoether ($C_{12}E_8$) was added to a final concentration of 10 mM to disperse the viral and liposomal membranes.

FP exposure assay. Microtiter plates were coated with polyclonal anti-TBEV immunoglobulin G to capture native RSPs (0.5 μ g/ml E) in phosphate-buffered saline, pH 7.4, containing 2% lamb serum as described previously (34). The exposure of the FP was measured by the addition of biotinylated MAb A1 (FP-specific MAb) in MES buffer (50 mM MES, 100 mM NaCl) adjusted to the appropriate pH by titration with 1 N NaOH. After incubation for 1 h at 37°C, the bound MAb A1 was detected by using streptavidin-peroxidase (Sigma-Aldrich) (8).

Liposome coflotation assay. RSPs were mixed with liposomes (1 μ g E and 200 nmol lipids), acidified with 300 mM MES to yield a pH of 5.4, and incubated for 15 min at 37°C. The acidified samples were back neutralized to pH 8.0 by the addition of 150 mM TEA and adjusted to 0.6 ml 20% sucrose (wt/wt) in TAN buffer, pH 8.0 (50 mM triethanolamine, 100 mM NaCl). These samples were layered onto a 1-ml 50% sucrose cushion and overlaid with 1.4 ml of 15% sucrose and 1 ml 5% sucrose as described previously (8). Centrifugation was carried out for 2 h at 50,000 rpm at 4°C in a Beckman SW55 rotor. Fractions of 0.2 ml were collected by upward displacement using a Piston Gradient Fractionator (BioComp Instruments Inc.), and the amount of E protein in each fraction was determined by a quantitative four-layer ELISA (12).

E trimerization and trimer stability assays. The oligomeric state of E, after incubation of RSPs at acidic or neutral pH, was determined by sedimentation analysis as described previously (2, 8). RSPs (3 μ g) in TAN buffer, pH 8.0, were incubated for 10 min at pH 5.4 or 8.0 by the addition of 300 mM MES or TAN buffer, pH 8.0, respectively. Acidified samples were back neutralized with 150 mM TEA, and all samples were solubilized with 1% Triton X-100 for 1 h at room temperature. For thermostability experiments, RSPs were acidified and solubilized as described above before being incubated for 10 min at 37°C or 70°C (8). All samples were applied on top of 7 to 20% (wt/wt) continuous sucrose gradients containing 0.1% Triton X-100. Centrifugation was carried out at 38,000 rpm and 15°C for 20 h in a Beckmann SW40 rotor. Fractions of 0.6 ml were collected by upward displacement using a Piston Gradient Fractionator (BioComp Instruments Inc.). The amount of E in the fractions was determined by a quantitative four-layer ELISA (12).

TABLE 1. Quality controls of TBEV WT and mutant RSPs

RSP	Reactivity with monoclonal antibodies	Oligomeric state of E	Hemagglutination activity	Particulate nature (ultracentrifugation)	Maturation cleavage
WT	+	Dimer	+	+	+
Δ TM2	+	Dimer	+	+	+
CT-Marburg	+	Dimer	+	+	+
CT-Synthetic	+	Dimer	+	+	+
JE1-JE2	+	Dimer	+	+	+
TBE1-JE2	+	Dimer	+	+	+
JE1-TBE2	+	Dimer	+	+	+

Immunofluorescence. RNA-transfected or virus-infected BHK-21 cells were seeded in 24-well tissue culture plates containing microscope coverslips and incubated for 24 h at 37°C. The cells were fixed and permeabilized with acetone-methanol (1:1) as described previously (39). Staining was performed by successive incubations with a rabbit polyclonal anti-TBEV serum recognizing the structural proteins and a fluorescein-isothiocyanate-conjugated anti-rabbit antibody (Jackson Immune Research Laboratory).

Focus formation assay. Supernatants from transfected BHK-21 cells were harvested 2 days postelectroporation and added to confluent cell monolayers in serial 10-fold dilutions. After 3 h of incubation at 37°C, the cells were covered with a 3% carboxymethyl cellulose overlay. Two days after infection, the cells were fixed and permeabilized with acetone-methanol (1:1) for 10 min at -20°C and incubated with a polyclonal rabbit anti-TBEV serum. Antibody-labeled cells were detected with goat anti-rabbit immunoglobulin G-alkaline phosphatase (Sigma-Aldrich).

RESULTS

RSP mutagenesis. We used the TBEV RSP system to investigate the effects of TMD modifications on the different steps of the flavivirus membrane fusion process. For this purpose, we generated mutant RSPs with modifications of the TM hairpin as follows (Fig. 1C): (i) deletion of the TM2 helix (Δ TM2); (ii) replacement of the TM2 helix by the carboxy-terminal tail of the Marburg virus fusion protein (CT-Marburg) or an oligo(R) tail (CT-Synthetic); (iii) replacement of the complete TM hairpin by the heterologous TM hairpin of JEV, a distantly related flavivirus (JE1-JE2); (iv) generation of a chimeric hairpin in which the TM2 domain was replaced by that of JEV (TBE1-JE2); or (v) generation of a chimeric hairpin in which the TM1 domain was replaced by that of JEV (JE1-TBE2).

Since the modification of the membrane anchor could potentially interfere with processes unrelated to fusion, we performed a series of quality control experiments to ensure WT-like folding and oligomerization of E, as well as particle formation and maturation of RSPs. The data from these analyses are summarized in Table 1. None of the introduced mutations affected the proper folding of E, as shown by reactivity with conformation-sensitive monoclonal antibodies (see Materials and Methods). The dimeric state of E was confirmed by sedimentation analysis after solubilization of RSPs with Triton X-100 (see Materials and Methods). The particulate organization of the mutants was verified by ultracentrifugation. Western blots using prM-specific polyclonal sera revealed that the maturation state of the mutants was identical to that of the WT control.

The TM hairpin is required for efficient membrane fusion. To assess the requirement for the TM2 domain in the overall fusion process, we used an *in vitro* lipid-mixing assay with

pyrene-labeled particles and liposomes (see Materials and Methods). Deletion of the TM2 helix resulted in strong impairment of the rate and extent of acidic-pH-induced fusion compared to the WT control (Fig. 2A). The addition of carboxy-terminal tails to the TM1 helix as a replacement for the TM2 helix (making E more similar to other viral fusion proteins) did not exert a compensating effect on fusion (Fig. 2B). RSPs containing E with either the cytoplasmic tail of the Marburg virus fusion protein or a synthetic poly(R) tail were even more impaired in membrane fusion than RSP Δ TM2. Further information about the contribution of the TM hairpin to membrane fusion was obtained by analyzing RSPs with a completely heterologous TM hairpin (JE1-JE2) and chimeric hairpins (TBE1-JE2 and JE1-TBE2) in E. RSP JE1-JE2 displayed virtually the same fusion characteristics as the WT with respect to the rate, as well as the extent, of fusion (Fig. 2C). In contrast, chimerization of the hairpin resulted in impairment, but not loss, of fusion activity (Fig. 2C). The quantitative evaluation of the effects of all TMD modifications on the extent of fusion relative to the WT are displayed in Fig. 2D.

From these experiments, we conclude that (i) the TM hairpin of E represents a functional element in the fusion process, (ii) the deletion of the TM2 helix cannot be compensated for by cytoplasmic tails, (iii) a heterologous flavivirus membrane anchor can completely substitute for the functions of the homologous TM hairpin in fusion, and (iv) mutants with chimeric anchors display fusion activities that are intermediate between the WT and Δ TM2. Since the highest fusion extents were achieved by RSPs with TM anchors containing matching helices (RSP WT and RSP JE1-JE2), it can be assumed that interactions between the TM1 and TM2 helices contribute to efficient fusion.

The TM hairpin is not required for early steps of membrane fusion. The fusion experiments revealed an important role of the TM2 helix and TM1-TM2 helix interactions in the overall process. However, it remained unclear for which stage of fusion these interactions were required. We therefore employed an experimental design that allowed us to dissect the fusion process and to specifically study the stages of fusion initiation, i.e., acidic-pH-induced FP exposure by the use of an FP-specific monoclonal antibody (MAb A1) in ELISA and interactions with target membranes by liposome coflotation. As shown in Fig. 3A, the deletion of TM2 had no measurable effect on the pH threshold and the extent of FP exposure. Also, the patterns of acidic-pH-induced liposome coflotation were virtually superimposable for RSP WT and RSP Δ TM2 (Fig. 3B). Consistent with the fusion assays, the use of pyrene-

T1/AQ:A

F2

F3

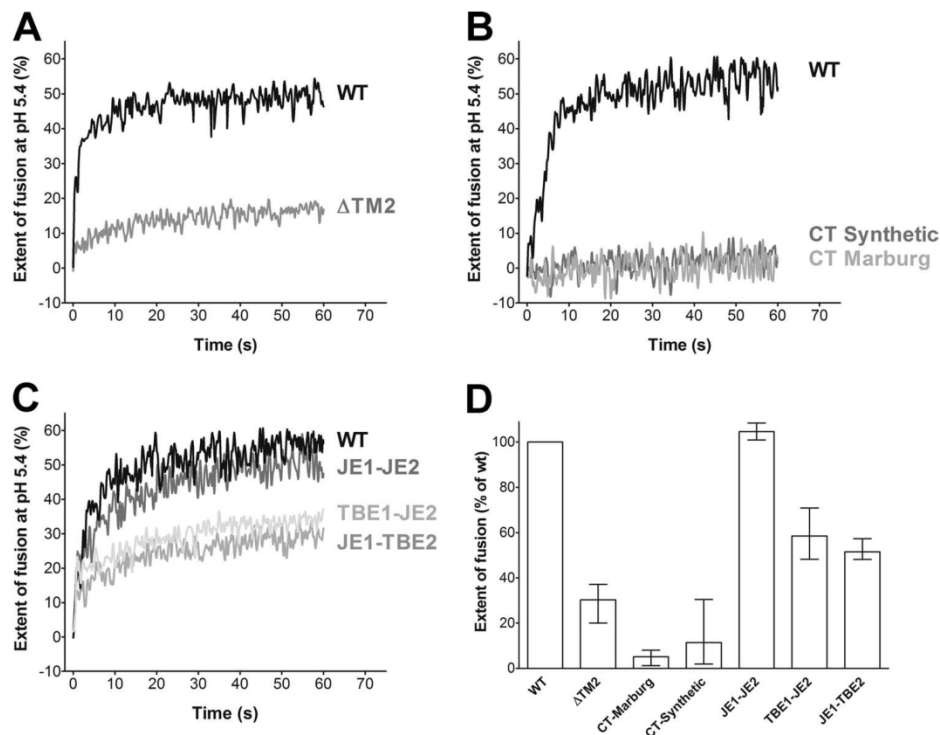


FIG. 2. Fusion activities of pyrene-labeled WT and mutant RSPs. (A) Fusion kinetics of RSP WT (black line) and Δ TM2 (gray line) at pH 5.4. (B) Fusion kinetics of RSP WT (black line) and RSPs in which the second TMD of E was replaced by a cytoplasmic tail (gray lines) at pH 5.4. (C) Fusion kinetics of RSP WT (black line) and RSPs with heterologous or shuffled E membrane anchors (gray lines) at pH 5.4. (D) Extent of fusion of mutant RSPs relative to RSP WT (= 100%) at pH 5.4 after 60 s. The data represent the means of at least two independent experiments, and the error bars indicate the observed range.

labeled RSPs in coflotation experiments confirmed that Δ TM2 RSPs were mostly attached to, but not fused with, liposomes (Fig. 3B, inset). The same results were also obtained with the other TM mutant RSPs, none of which were affected in their association with liposomes at acidic pH (Fig. 3C).

These data indicate that the second TM helix is fully dispensable for the early stages of membrane fusion and that the membrane anchorage of E by the TM1 helix alone is sufficient for the exposure of the FP, as well as its insertion into target membranes.

Reduced thermostability of trimers lacking the TM2 helix.

Since the deletion of the TM2 helix did not affect the initiation of fusion, the block observed with this mutant in overall fusion must occur at later stages of the multistep fusion process. Trimerization and the conformational switch from the prefusion into the postfusion conformation of E represent crucial events in the fusion process and are believed to provide the energy for merging the two membranes. We therefore analyzed the effects of TMD modifications on trimer formation (Fig. 4) and trimer stability (Fig. 5).

As revealed by rate zonal centrifugation of low-pH-pretreated and solubilized RSPs, all mutant E proteins were able to undergo the dimer-to-trimer transition similarly to the WT (Fig. 4A and B). A slight reduction in the efficiency of trimerization was observed with the constructs carrying carboxy-terminal tails, indicating that the added sequence elements somehow interfered with the formation of trimers (Fig. 4B).

The stability of the mutant E trimers was investigated in thermal denaturation experiments. After low-pH pretreatment and solubilization of RSPs, the samples were heated, and the effect on the oligomeric state of the solubilized E trimers was analyzed by sedimentation in sucrose gradients. As shown in Fig. 5A and B, the WT trimers were stable up to 70°C but started to denature and aggregate at about 75°C (data not shown). Mutant trimers containing a double membrane anchor (both heterologous and chimeric anchors) displayed stability similar to that of the WT and were found to sediment in the corresponding fractions in sucrose gradients (Fig. 5A). In contrast, the deletion of the TM2 helix or its replacement by cytoplasmic tails resulted in a reduction of thermostability, as revealed by a strong aggregation of E trimers at 70°C and sedimentation of most of the material into the pellet at the bottom of the gradients (Fig. 5B).

In conclusion, these data show that the TM2 helix is dispensable for trimer formation but contributes to interactions that stabilize the postfusion trimer.

Heterologous and chimeric anchors strongly reduce the production of virus particles. We attempted to assess the significance of the observations made with RSP TM mutants also in the context of infectious virions and therefore engineered heterologous and chimeric membrane anchors (JE1-JE2, TBE1-JE2, and JE1-TBE2) into an infectious cDNA clone of TBEV. Since the TM2 element is indispensable for polyprotein translation and thus for the generation of infectious virions (Fig.

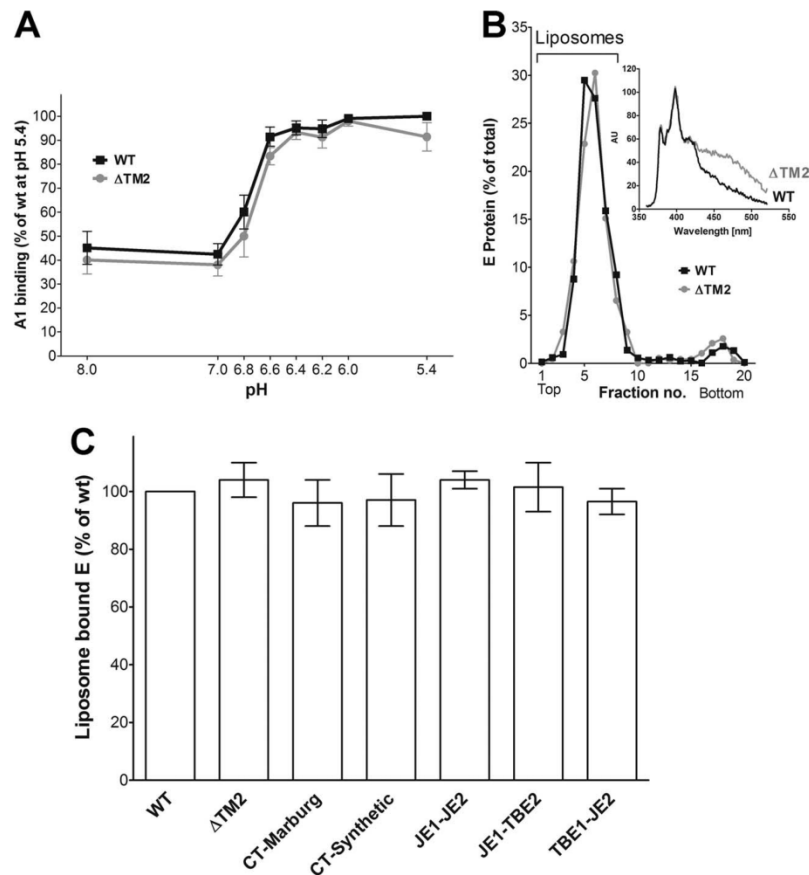


FIG. 3. Interactions of WT and mutant RSPs with target membranes. (A) Acidic-pH-induced FP exposure measured by binding of MAb A1. The results are expressed as percentages of the maximal absorbance of A1 obtained with the WT at pH 5.4. The data are the means of four independent experiments performed in duplicate, and the error bars indicate the standard errors of the means. WT, squares; Δ TM2, circles. (B) Acidic-pH-induced coflotation of WT and Δ TM2 RSPs with liposomes. The top fractions containing RSPs coflotated with the liposomes are indicated by a bracket. (Inset) Fluorescence spectrum of coflotated pyrene-labeled mutant (gray) and WT (black) RSPs. AU, arbitrary units. (C) Extent of acidic-pH-induced coflotation with liposomes obtained with mutant RSPs relative to the WT (= 100%). The data are the means of two independent experiments; the error bars indicate the observed range.

1A), a Δ TM2 mutant could not be analyzed in this part of the study.

Immunofluorescence staining of transfected cells did not reveal any differences between WT and mutant viruses (Fig. 6A). To determine whether the transfected cells not only produced viral proteins but also released infectious virions, the cell culture supernatants of the experiments displayed in Fig. 6A were transferred to fresh cells, which were stained after 24 h. As can be seen from Fig. 6B, only a few positive cells were detected in the case of the mutants in contrast to the WT control. Quantification of the primary cell culture supernatants (Fig. 6A) by focus formation assays showed that the infectious titers of the mutant viruses were at least $\sim 10,000$ -fold lower than that of the WT control (Fig. 6C). A comparative analysis of RNA equivalents in these supernatants revealed that the specific infectivities of the mutants were also dramatically reduced (Fig. 6D).

Due to these low yields of mutant viruses, it was not possible to produce the amounts of virus necessary for the biochemical analyses conducted with RSPs.

DISCUSSION

The double-membrane-spanning C-terminal anchor (TM1 and TM2) of the envelope protein E (consisting of two anti-parallel helices) is a unique distinguishing structural feature of the flavivirus fusion protein E. The TM2 helix is a remnant of flavivirus polyprotein processing and has an essential function, serving as an internal signal sequence for the synthesis of the first nonstructural protein, NS1 (Fig. 1A) (21). All other viral fusion proteins analyzed so far have single TM anchors that are C-terminally extended by intracytoplasmic tails of various lengths (41). With class I and III fusion proteins, it was shown in several studies that TMD modifications affected late stages of membrane fusion, such as the hemifusion state and/or the opening of the fusion pore (reviewed in references 20 and 41). We demonstrate in this work, using virus-like particles of TBEV as a model system, that the flavivirus TM2 helix is apparently multifunctional and not only essential for viral polyprotein processing, but also indispensable for efficient membrane fusion.

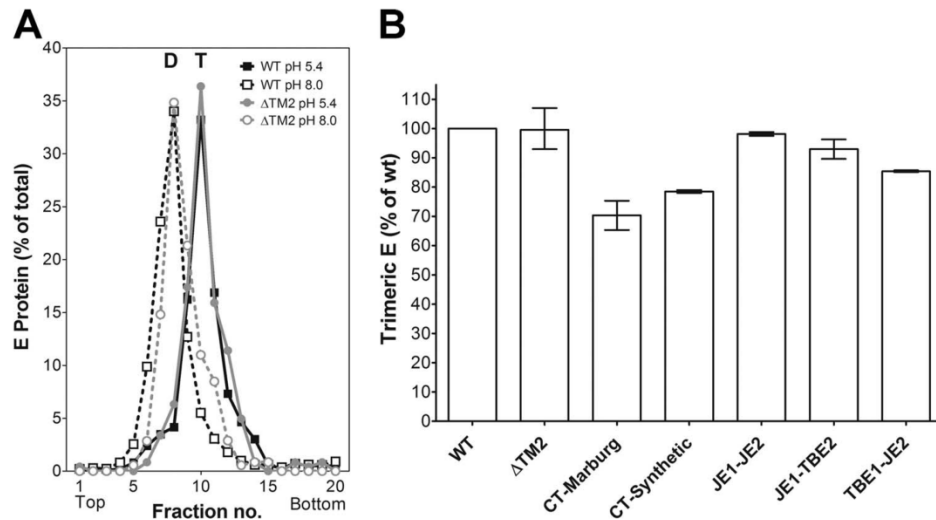


FIG. 4. E trimer formation of WT and mutant RSPs. Analysis of acidic-pH-induced trimer formation by sucrose gradient centrifugation, as described in Materials and Methods, after Triton X-100 solubilization of acidic-pH-pretreated and untreated RSPs. (A) Sedimentation patterns of E from RSP Δ TM2 (gray lines) and RSP WT (black lines). Dotted lines, untreated RSPs; solid lines, acidic-pH-treated RSPs. The sedimentation direction is from left to right, and the positions of E dimers (D) and trimers (T) are indicated. (B) Extent of E trimer formation obtained with mutant RSPs compared to the WT (= 100%). The results are expressed as percentages of E found in the trimer peak fractions relative to the total amount of E in the gradient. The data represent the means of at least two independent experiments, and the error bars indicate the observed range.

It is an important finding of our study that all of the initial steps of flavivirus fusion (i.e., acidic-pH-induced dissociation of E, FP exposure, and its interaction with target membranes) can proceed completely unimpaired in the absence of the TM2 helix, whereas later steps leading to hemifusion and full fusion are blocked. In the current models (11, 14, 36), these later

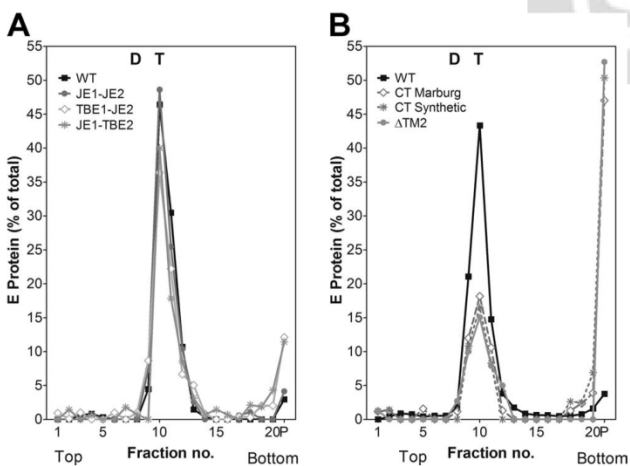


FIG. 5. Thermostability of E trimers of WT and mutant RSPs. Acidic-pH-induced E trimers of WT and mutant RSPs were exposed to 70°C and subjected to rate zonal sucrose density gradient centrifugation. The sedimentation direction is from left to right, and the positions of E dimers (D) and trimers (T) are indicated. The pellet (P) was resuspended in 0.6 ml, corresponding to the volume of a single fraction. (A) JE1-JE2, TBE1-JE2, and JE1-TBE2 mutant trimers, displaying trimer stability similar to that of the WT. (B) Δ TM2, CT-Marburg, and CT-Synthetic mutant trimers displaying strongly reduced thermostability compared to the WT. The data are representative examples from two or more independent experiments.

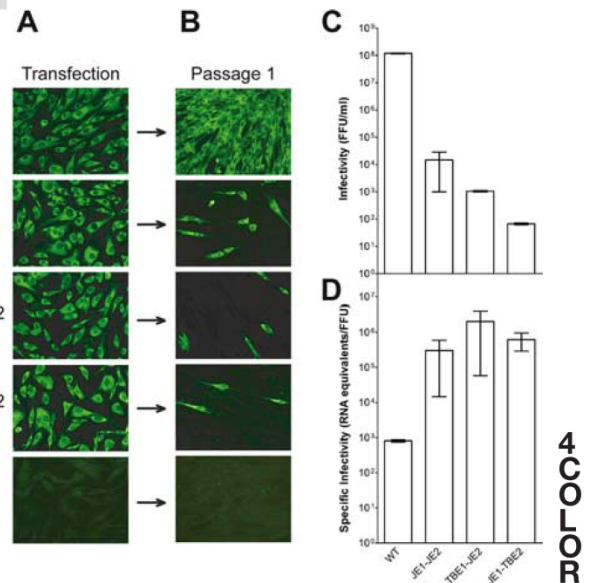


FIG. 6. Infectivity of TMD virus mutants. (A) Immunofluorescence staining of BHK cells transfected with mutant or WT viral RNAs, as indicated on the left. (B) Immunofluorescence staining of cells infected with the supernatants from panel A harvested 48 h after transfection. Staining was carried out using a polyclonal serum recognizing the structural proteins of TBEV. The data are representative examples from two or more independent experiments. (C) Quantification of virus in the cell culture supernatants of panel A harvested 48 h after transfection by focus formation assays. FFU, focus-forming units. (D) Determination of the specific infectivities (RNA equivalents per infectious unit) of virus in the cell culture supernatants of panel A harvested 48 h after transfection. Two independent experiments were carried out in duplicate. The data represent the means of these two experiments, and the error bars indicate the observed range.

steps include the trimerization of E and its conversion into an energetically more stable postfusion conformation, as well as possible further protein-protein interactions. Together, these structural changes and interactions are believed to provide the energy necessary for merging the two membranes and the formation of a fusion pore (Fig. 1B). Since the replacement of both TBEV TMDs with those from the distantly related flavivirus JEV did not impair fusion activity, it can be assumed that intra- and/or interprotein interactions between the TM helices are essential for flavivirus fusion. Such interactions clearly contribute to trimer stability, because all trimers lacking the TM2 domain were significantly less thermostable than trimers with both TM helices. WT-like trimer stability, however, is apparently not dependent on a homologous match between the two TM helices, because the mutants with chimeric TM hairpins, derived from TBEV and JEV, displayed a trimer stability phenotype similar to that of the WT. It is therefore justified to assume that interactions between homologous TM2 helices contribute to the stability of the postfusion trimer. Despite this unimpaired trimer stability, the overall fusion activity of RSPs with chimeric TM hairpins was reduced compared to those with homologous TM hairpins, suggesting an additional functional role of the TM helices in fusion. One likely possibility is that they also contribute to intertrimer interactions involved in the formation of higher-order structures at the site of fusion pore formation. Such ring-like clusters of interacting fusion proteins have been proposed to form during the process of alphavirus fusion (9), i.e., for another family of icosahedral enveloped viruses with class II fusion proteins, like flaviviruses.

It must be kept in mind that the structural details of the interactions of the TM1 and TM2 helices within the anchor and with other parts of E are not known for the postfusion conformation of E. The crystal structures of truncated sE trimers of TBEV and dengue virus, however, indicate a juxtaposition of the TM hairpin and the FPs on the same side of the molecule (4, 26, 29). Therefore, interactions not only between the two helices within the anchor, but also of the TM anchor with the FPs, might contribute to fusion (38). The short loop connecting the two TM helices is unlikely to be important for these interactions, because the TM1-TM2 chimeras, which contained either a TM1 loop or a TM2 loop match, behaved identically in all our analyses.

Given the structural similarity of alphavirus and flavivirus fusion proteins (15, 32), their difference with respect to the membrane anchors—single TM and double TM anchors, respectively—is noteworthy, especially when the essential role of the TM2 helix for flavivirus fusion is considered. Inspection of the alphavirus particle, however, reveals that there are other TMDs that could serve functions similar to that of the flavivirus TM2 helix and provide interactions that contribute to efficient fusion. First, the TM segments of the two envelope proteins E1 and E2 are strongly intertwined (22, 28), and it has been suggested that these interactions exert a cooperative effect at an as yet undefined step of alphavirus membrane fusion (42). This is in strong contrast to the TM regions of the two envelope proteins of flaviviruses (prM/M and E), which were shown by cryo-EM to be separate and not to interact (45). Second, alphavirus particles contain the 6K protein, a remnant of polyprotein processing, which appears to contribute significantly to the efficiency of alphavirus fusion (25). Experiments

with recombinant viruses lacking 6K showed that they were strongly impaired in fusion activity (25), very much like the Δ TM2 mutants in our work. It can therefore be speculated that E1-6K interactions during alphavirus fusion are related to those of the TM1 and TM2 helices in the case of flaviviruses.

The engineering of recombinant TBEV with completely heterologous TM anchors or chimeric TM anchors resulted in a dramatic reduction of specific infectivities (RNA equivalents to focus-forming units) and a severe impairment of virus growth (Fig. 6C and D), prohibiting the production of sufficient amounts of mutant viruses that would have been necessary for conducting fusion experiments similar to those presented for RSPs. There are different possible, not mutually exclusive explanations for these findings. In the case of the chimeric TM hairpin mutants, reduced fusion activities, as observed with the RSPs, could contribute to the low infectivities. However, the specific infectivity of the JE1-JE2 mutants was also strongly reduced and led to 10,000-times-lower yields than the WT, although the same mutation had no effect on fusion activity in the RSP system. It therefore must be assumed that modifications of the TM helices in the virus also affected other steps of virus replication, independent of membrane fusion. Particle assembly would be a primary candidate for such effects, involving mechanisms that contribute to virion, but not to subviral particle, formation. RSPs can be formed through lateral interactions between prM-E heterodimers only, and they are smaller than whole virions (33). In mature RSPs, the E homodimers are arranged in a regular $T = 1$ icosahedral lattice (7), whereas on the virus surface, the E proteins are more tightly packed in a herringbone-like arrangement (19, 27). It is possible that the more complex organization of the viral envelope requires interactions of the TMDs of prM-E heterodimers during assembly and/or budding that are dispensable for RSP formation. Such an interpretation would be consistent with other studies that had revealed that alterations in the membrane anchor of E could severely impair the production of infectious viruses (13, 30, 31).

Irrespective of the possible involvement of the TM helices of E in virus assembly, our data provide evidence that they play an important role in the late stages of flavivirus membrane fusion and provide both intra- and intermolecular E trimer contacts that are necessary to drive the fusion process to completion. This is an extension of existing models of flavivirus fusion that have focused on the relocation of DIII and the zippering of the stem to serve as primary energy sources for this process (11).

ACKNOWLEDGMENTS

This work was supported by the Austrian Science Fund (FWF) (P19843-B13 and P20533-B03).

We thank Cornelia Stöckl for excellent technical assistance and Harald Rouha for help with the quantitative-PCR experiments.

REFERENCES

- Allison, S. L., C. W. Mandl, C. Kunz, and F. X. Heinz. 1994. Expression of cloned envelope protein genes from the flavivirus tick-borne encephalitis virus in mammalian cells and random mutagenesis by PCR. *Virus Genes* 8:187–198.
- Allison, S. L., J. Schlich, K. Stiasny, C. W. Mandl, and F. X. Heinz. 2001. Mutational evidence for an internal fusion peptide in flavivirus envelope protein E. *J. Virol.* 75:4268–4275.
- Allison, S. L., K. Stiasny, K. Stadler, C. W. Mandl, and F. X. Heinz. 1999. Mapping of functional elements in the stem-anchor region of tick-borne encephalitis virus envelope protein E. *J. Virol.* 73:5605–5612.

4. Bressanelli, S., et al. 2004. Structure of a flavivirus envelope glycoprotein in its low-pH-induced membrane fusion conformation. *EMBO J.* **23**:728–738.
5. Clarke, D. H., and J. Casals. 1958. Techniques for hemagglutination and hemagglutination-inhibition with arthropod-borne viruses. *Am. J. Trop. Med. Hyg.* **7**:561–573.
6. Corver, J., et al. 2000. Membrane fusion activity of tick-borne encephalitis virus and recombinant subviral particles in a liposomal model system. *Virology* **269**:37–46.
7. Ferlenghi, L., et al. 2001. Molecular organization of a recombinant subviral particle from tick-borne encephalitis virus. *Mol. Cell* **7**:593–602.
8. Fritz, R., K. Stiasny, and F. X. Heinz. 2008. Identification of specific histidines as pH sensors in flavivirus membrane fusion. *J. Cell Biol.* **183**:353–361.
9. Gibbons, D. L., et al. 2004. Conformational change and protein-protein interactions of the fusion protein of Semliki Forest virus. *Nature* **427**:320–325.
10. Gubler, D., G. Kuno, and L. Markhoff. 2007. Flaviviruses, p. 1153–1252. *In* D. M. Knipe, P. M. Howley, D. E. Griffin, R. A. Lamb, M. A. Martin, B. Roizman, and S. E. Straus (ed.), *Fields virology*, 5th ed. Lippincott, Williams & Wilkins, Philadelphia, PA.
11. Harrison, S. C. 2008. Viral membrane fusion. *Nat. Struct. Mol. Biol.* **15**:690–698.
12. Heinz, F. X., et al. 1994. Structural changes and functional control of the tick-borne encephalitis virus glycoprotein E by the heterodimeric association with protein prM. *Virology* **198**:109–117.
13. Hsieh, S. C., W. Y. Tsai, and W. K. Wang. 2010. The length of and nonhydrophobic residues in the transmembrane domain of dengue virus envelope protein are critical for its retention and assembly in the endoplasmic reticulum. *J. Virol.* **84**:4782–4797.
14. Kaufmann, B., and M. G. Rossmann. 2010. Molecular mechanisms involved in the early steps of flavivirus cell entry. *Microbes Infect.* **13**:1–9.
15. Kielian, M., and F. A. Rey. 2006. Virus membrane-fusion proteins: more than one way to make a hairpin. *Nat. Rev. Microbiol.* **4**:67–76.
16. Kiermayr, S., K. Stiasny, and F. X. Heinz. 2009. Impact of quaternary organization on the antigenic structure of the tick-borne encephalitis virus envelope glycoprotein E. *J. Virol.* **83**:8482–8491.
17. Kofler, R. M., F. X. Heinz, and C. W. Mandl. 2002. Capsid protein C of tick-borne encephalitis virus tolerates large internal deletions and is a favorable target for attenuation of virulence. *J. Virol.* **76**:3534–3543.
18. Kofler, R. M., V. M. Hoenninger, C. Thurner, and C. W. Mandl. 2006. Functional analysis of the tick-borne encephalitis virus cyclization elements indicates major differences between mosquito-borne and tick-borne flaviviruses. *J. Virol.* **80**:4099–4113.
19. Kuhn, R. J., et al. 2002. Structure of dengue virus: implications for flavivirus organization, maturation, and fusion. *Cell* **108**:717–725.
20. Langosch, D., M. Hofmann, and C. Ungermann. 2007. The role of transmembrane domains in membrane fusion. *Cell. Mol. Life Sci.* **64**:850–864.
21. Lindenbach, B. D., H. J. Thiel, and C. M. Rice. 2007. *Flaviviridae: the viruses and their replication*, p. 1101–1152. *In* D. M. Knipe, P. M. Howley, D. E. Griffin, R. A. Lamb, M. A. Martin, B. Roizman, and S. E. Straus (ed.), *Fields virology*, 5th ed. Lippincott, Williams & Wilkins, Philadelphia, PA.
22. Mancini, E. J., M. Clarke, B. E. Gowen, T. Rutten, and S. D. Fuller. 2000. Cryo-electron microscopy reveals the functional organization of an enveloped virus, Semliki Forest virus. *Mol. Cell* **5**:255–266.
23. Mandl, C. W., M. Ecker, H. Holzmann, C. Kunz, and F. X. Heinz. 1997. Infectious cDNA clones of tick-borne encephalitis virus European subtype prototypic strain Neudoerfl and high virulence strain Hypr. *J. Gen. Virol.* **78**:1049–1057.
24. Martens, S., and H. T. McMahon. 2008. Mechanisms of membrane fusion: disparate players and common principles. *Nat. Rev. Mol. Cell Biol.* **9**:543–556.
25. McInerney, G. M., J. M. Smit, P. Liljestrom, and J. Wilschut. 2004. Semliki Forest virus produced in the absence of the 6K protein has an altered spike structure as revealed by decreased membrane fusion capacity. *Virology* **325**:200–206.
26. Modis, Y., S. Ogata, D. Clements, and S. C. Harrison. 2004. Structure of the dengue virus envelope protein after membrane fusion. *Nature* **427**:313–319.
27. Mukhopadhyay, S., B. S. Kim, P. R. Chipman, M. G. Rossmann, and R. J. Kuhn. 2003. Structure of West Nile virus. *Science* **302**:248.
28. Mukhopadhyay, S., et al. 2006. Mapping the structure and function of the E1 and E2 glycoproteins in alphaviruses. *Structure* **14**:63–73.
29. Nayak, V., et al. 2009. Crystal structure of dengue virus type 1 envelope protein in the postfusion conformation and its implications for membrane fusion. *J. Virol.* **83**:4338–4344.
30. Op De Beeck, A., et al. 2003. Role of the transmembrane domains of prM and E proteins in the formation of yellow fever virus envelope. *J. Virol.* **77**:813–820.
31. Orlinger, K. K., V. M. Hoenninger, R. M. Kofler, and C. W. Mandl. 2006. Construction and mutagenesis of an artificial bicistronic tick-borne encephalitis virus genome reveals an essential function of the second transmembrane region of protein E in flavivirus assembly. *J. Virol.* **80**:12197–12208.
32. Sánchez-San Martín, C., C. Y. Liu, and M. Kielian. 2009. Dealing with low pH: entry and exit of alphaviruses and flaviviruses. *Trends Microbiol.* **17**:514–521.
33. Schalich, J., et al. 1996. Recombinant subviral particles from tick-borne encephalitis virus are fusogenic and provide a model system for studying flavivirus envelope glycoprotein functions. *J. Virol.* **70**:4549–4557.
34. Stiasny, K., S. Brandler, C. Kossel, and F. X. Heinz. 2007. Probing the flavivirus membrane fusion mechanism by using monoclonal antibodies. *J. Virol.* **81**:11526–11531.
35. Stiasny, K., R. Fritz, K. Pangerl, and F. X. Heinz. 2009. Molecular mechanisms of flavivirus membrane fusion. *Amino Acids*. doi:10.1007/s00726-009-0370-4.
36. Stiasny, K., and F. X. Heinz. 2006. Flavivirus membrane fusion. *J. Gen. Virol.* **87**:2755–2766.
37. Stiasny, K., C. Koessl, and F. X. Heinz. 2003. Involvement of lipids in different steps of the flavivirus fusion mechanism. *J. Virol.* **77**:7856–7862.
38. Sultana, H., et al. 2009. Fusion loop peptide of the West Nile virus envelope protein is essential for pathogenesis and is recognized by a therapeutic cross-reactive human monoclonal antibody. *J. Immunol.* **183**:650–660.
39. Taucher, C., A. Berger, and C. W. Mandl. 2010. A trans-complementing recombination trap demonstrates a low propensity of flaviviruses for intermolecular recombination. *J. Virol.* **84**:599–611.
40. Thiel, H. J., et al. 2005. Family Flaviviridae, p. 981–998. *In* C. M. Fauquet, M. A. Mayo, J. Maniloff, U. Desselberger, and L. A. Ball (ed.), *Virus taxonomy*. Eighth report of the International Committee on Taxonomy of Viruses. Elsevier Academic Press, San Diego, CA.
41. White, J. M., S. E. Delos, M. Brecher, and K. Schornberg. 2008. Structures and mechanisms of viral membrane fusion proteins: multiple variations on a common theme. *Crit. Rev. Biochem. Mol. Biol.* **43**:189–219.
42. Wu, S. R., et al. 2007. The dynamic envelope of a fusion class II virus. Prefusion stages of semliki forest virus revealed by electron cryomicroscopy. *J. Biol. Chem.* **282**:6752–6762.
43. Yu, I. M., et al. 2009. Association of the pr peptides with dengue virus at acidic pH blocks membrane fusion. *J. Virol.* **83**:12101–12107.
44. Yu, I. M., et al. 2008. Structure of the immature dengue virus at low pH primes proteolytic maturation. *Science* **319**:1834–1837.
45. Zhang, W., et al. 2003. Visualization of membrane protein domains by cryo-electron microscopy of dengue virus. *Nat. Struct. Biol.* **10**:907–912.

Curriculum Vitae

Janja Blazevic

Persönliche Daten:

Geburtsdatum: 11.06.1984

Geburtsort: Brcko, Bosnien und Herzegowina

Staatsbürgerschaft: Österreich

Ausbildung:

1990-1994 Volksschule, Wien

1994-1998 musisch-kreative Hauptschule, Wien

1998-2003 Höhere Bundeslehr- und Versuchsanstalt für chemische Industrie, Wien

Matura im Juni 2003 mit ausgezeichnetem Erfolg

Diplomarbeit bei Baxter AG: „Virusreduktion durch Herstellprozesse von medizinischen Plasmaderivaten“

2004-2011 Studium der Molekularen Biologie an der Universität Wien

2009-2011 Diplomarbeit am Department für Virologie

Praktika:

07/2000-08/2000 Vienna Lab GmbH

07/2001 Vienna Lab GmbH

07/2006-09/2006 Boehringer Ingelheim Austria GmbH

07/2007-08/2007 Boehringer Ingelheim Austria GmbH

07/2008 Boehringer Ingelheim Austria GmbH

Arbeitserfahrung:

08/2003-10/2004 Nano-S Biotechnologie GmbH

Publikation:

Journal of Virology: „The unique transmembrane hairpin of the flavivirus fusion protein E is essential for membrane fusion.“ Fritz R, Blazevic J, Taucher C, Pangerl K, Heinz FX, Stiasny K.; paper in press